

1 TITLE PAGE

2

3 **Evaluating the effects of China's pollution controls on inter-annual**  
4 **trends and uncertainties of atmospheric mercury emissions**

5

6 Yu Zhao<sup>1,2\*</sup>, Hui Zhong<sup>1</sup>, Jie Zhang<sup>2,3</sup>, Chris P. Nielsen<sup>4</sup>

7

8 1. State Key Laboratory of Pollution Control & Resource Reuse and School of the Environment,  
9 Nanjing University, 163 Xianlin Ave., Nanjing, Jiangsu 210023, China

10 2. Collaborative Innovation Center of Atmospheric Environment and Equipment Technology,  
11 CICAET, Nanjing, Jiangsu 210044, China

12 3. Jiangsu Provincial Academy of Environmental Science, 176 North Jiangdong Rd., Nanjing, Jiangsu  
13 210036, China

14 4. Harvard China Project, School of Engineering and Applied Sciences, Harvard University, 29  
15 Oxford St, Cambridge, MA 02138, USA

16

17 \*Corresponding author: Yu Zhao

18 Phone: 86-25-89680650; email: [yuzhao@nju.edu.cn](mailto:yuzhao@nju.edu.cn)

19 **ABSTRACT**

20 China's anthropogenic emissions of atmospheric mercury (Hg) are effectively constrained by  
21 national air pollution control and energy efficiency policies. In this study, improved methods, based  
22 on available data from domestic field measurements, are developed to quantify the benefits of Hg  
23 abatement by various emission control measures. Those measures include increased use of (1) flue  
24 gas desulfurization (FGD) and selective catalyst reduction (SCR) systems in power generation; (2)  
25 precalciner kilns with fabric filters (FF) in cement production; (3) mechanized coking ovens with  
26 electrostatic precipitators (ESP) in iron & steel production; and (4) advanced production technologies  
27 in nonferrous metal smelting. Investigation reveals declining trends in emission factors for each of  
28 these sources, which together drive a much slower growth of total Hg emissions than the growth of  
29 China's energy consumption and economy, from 679 metric tons (t) in 2005 to 750 t in 2012. In  
30 particular, estimated emissions from the above-mentioned four source types declined 3% from 2005  
31 to 2012, which can be attributed to expanded deployment of technologies with higher energy  
32 efficiencies and air pollutant removal rates. Emissions from other anthropogenic sources are estimated  
33 to increase by 22% during the period. The species shares of total Hg emissions have been stable in  
34 recent years, with mass fractions of around 55%, 39%, and 6% for gaseous elemental Hg ( $\text{Hg}^0$ ),  
35 reactive gaseous mercury ( $\text{Hg}^{2+}$ ), and particle-bound mercury ( $\text{Hg}^p$ ), respectively. The higher estimate  
36 of total Hg emissions than previous inventories is supported by limited simulation of atmospheric  
37 chemistry and transport. With improved implementation of emission controls and energy saving, a  
38 23% reduction in annual Hg emissions from 2012 to 2030, to below 600 t, is expected at the most.  
39 While growth in Hg emissions has been gradually constrained, uncertainties quantified by  
40 Monte-Carlo simulation for recent years have increased, particularly for the power sector and

41 particular industrial sources. The uncertainty (expressed as 95% confidence intervals) of Hg  
42 emissions from coal-fired power plants, for example, increased from -48%–+73% in 2005 to  
43 -50%–+89% in 2012. This is attributed mainly to increased penetration of advanced manufacturing  
44 and pollutant control technologies; the unclear operational status and relatively small sample sizes of  
45 field measurements of those processes have resulted in lower but highly varied emission factors. To  
46 reduce uncertainty and further confirm the benefits of pollution control and energy policies, therefore,  
47 systematic investigation of specific Hg pollution sources is recommended. The variability of temporal  
48 trends and spatial distributions of Hg emissions need to be better tracked during the ongoing dramatic  
49 changes in China's economy, energy use, and air pollution status.

50

## 51 **1 INTRODUCTION**

52 Increasing international efforts have been made to study and control the emissions of mercury  
53 (Hg), a pollutant well-known for its toxicity and long-range transport. Atmospheric emissions are  
54 identified as the most significant pathway of Hg release into the environment (Pirrone and Mason,  
55 2009). In contrast to other heavy metals that are mainly associated with air particles, atmospheric Hg  
56 includes several forms: gaseous elemental Hg (GEM,  $\text{Hg}^0$ ), which has the longest atmospheric  
57 lifetime and transport distance; reactive gaseous mercury (RGM,  $\text{Hg}^{2+}$ ), which is generally derived  
58 from more local sources; and particle-bound mercury (PBM,  $\text{Hg}^p$ ).

59 Available global emission inventories indicate that China has become the highest ranking nation  
60 in anthropogenic Hg emissions, attributed mainly to intensive use of fossil fuels to serve a large and  
61 rapidly growing economy (Fu et al., 2012a; Pacyna et al., 2010; Pirrone et al., 2010). Pacyna et al.  
62 (2010) calculated China's Hg emissions from fossil fuel use at 400 metric tons (t) in 2005, almost half

63 of the country's anthropogenic emissions. Domestic field measurements or investigations of Hg  
64 emissions have also been conducted for other sources including cement production (Li, 2011), metals  
65 mining and smelting (P Li et al., 2009; Li et al., 2012; Li et al., 2010; Wang et al., 2010a; Wu et al.,  
66 2012), solid waste incineration (L Chen et al., 2013; Hu et al., 2012) and biomass burning (C Chen et  
67 al., 2013; Huang et al., 2011). Most current inventories, however, did not sufficiently consider the  
68 differences in application of technologies, or made full use of country- or region-dependent  
69 information related to emissions. Global emission factors were applied instead to many sectors. As  
70 stressed by AMAP/UNEP (2013), research on the industrial processes and technologies employed to  
71 reduce Hg emissions in different industries, and more importantly in specific countries, is a priority to  
72 improve estimation of Hg emissions.

73 Under strong pressure to improve air quality (and to strengthen energy security and limit carbon  
74 emissions), China's government has been implementing a series of measures to conserve energy and  
75 control emissions. Since 2005, for example, small and inefficient plants or boilers in the power sector  
76 and certain heavy industrial sectors including cement and steel production have been gradually  
77 replaced with larger, energy-efficient units that include advanced dust collectors. Installation of flue  
78 gas desulfurization (FGD) systems have been compulsory at all new thermal power units to abate SO<sub>2</sub>  
79 emissions, and the FGD penetration has increased from 13% of total thermal power capacity in 2005  
80 to 86% in 2010 (Zhao et al., 2008; 2013). Since 2010, selective catalyst reduction (SCR) systems have  
81 been increasingly installed in power plants to reduce NO<sub>x</sub> emissions, and the penetration is expected  
82 to rise from 10% in 2010 to 70% in 2015 (Wang, 2013). The 2013 announcement of a national action  
83 plan of air pollution control, responding to recent severe urban haze episodes, will result in further  
84 advances in emission abatement and air quality in the future (Zhao et al., 2014). Although designed to  
85 target other pollutants, all of these measures have ancillary benefits to atmospheric Hg abatement. For

86 example, the use of advanced dust collectors (e.g., fabric filters (FF) and electrostatic precipitators  
87 (ESP)) and FGD are expected to significantly reduce emission levels (USEPA, 2002a; Wang et al.,  
88 2010b). SCR catalysts convert part of the  $\text{Hg}^0$  to  $\text{Hg}^{2+}$ , which is more liable to be absorbed by the  
89 FGD scrubber (Wang et al., 2012; Tian et al., 2012). Failure to track and evaluate such swift changes  
90 in emission sources and control technologies will lead to less accurate estimates of the trends in  
91 China's Hg emissions and its contributions to the global Hg cycle. Currently, most global estimates of  
92 historical and future Hg emissions show steadily increasing trends, driven mainly by expansion of  
93 industry in Asia (Streets et al., 2009a; Driscoll et al., 2013; AMAP/UNEP, 2013). This is inconsistent,  
94 however, with declining worldwide trends in background atmospheric Hg concentrations (Slemr et al.,  
95 2011; Ci et al., 2012; Driscoll et al., 2013).

96       Aside from the implications of recent and future trends, the Hg emission uncertainties pose  
97 further problems to the scientific community. The uncertainties will be transferred by use of the  
98 emission estimates in atmospheric chemistry simulations to analyses of transport and deposition of Hg  
99 (Pan et al., 2008; Lin et al., 2010; Corbitt et al., 2011). Despite this, very few countries include  
100 quantified uncertainties in their national emission reporting, particularly developing countries with  
101 poorer data availability and quality including China (Pacyna et al., 2010; Ci et al., 2012;  
102 AMAP/UNEP, 2013). To date, only the uncertainties of emissions from the power sector have been  
103 systematically quantified for China (Wu et al., 2010), with the lack of estimates for other sectors  
104 attributed mainly to limited information about other emission source types.

105       This study therefore seeks to assess the effects of recently implemented and ongoing control  
106 measures on past and future inter-annual trends and sector distributions of China's anthropogenic Hg  
107 emissions. The uncertainty of emissions is quantified, and the most sensitive parameters identified for  
108 improvement of future estimates.

109

## 110 **2 METHODOLOGY AND DATA SOURCES**

### 111 **2.1 Brief summary of Hg emission estimation**

112 The research domain covers the 31 provinces of mainland China. Annual emissions of Hg,  
113 including speciated forms ( $\text{Hg}^0$ ,  $\text{Hg}^{2+}$ , and  $\text{Hg}^{\text{p}}$ ), are estimated at the provincial level from 2005 to  
114 2012, to evaluate the effects of China's energy policies and air pollution control measures. The main  
115 anthropogenic activities fall into three sector categories: coal-fired power plants (CPP), all other  
116 industrial facilities (IND), and the residential & commercial sector (RES). IND is further divided into  
117 cement kilns (CEM), iron & steel plants (ISP), heating boilers (HB), other industrial boilers (OIB),  
118 nonferrous metal smelting plants (NMS), gold mining operations (GM, including large-scale gold  
119 mining, LGM, and artisanal and small-scale gold mining, ASGM), and the operations of other  
120 miscellaneous processes (OMP). RES mainly includes coal combustion (RC), oil & gas combustion  
121 (ROG), biofuel use/biomass open burning (BIO), and solid waste incineration (SWI) subcategories.  
122 As the dominant primary energy resource, coal plays important roles in most anthropogenic pollutant  
123 emissions in China (Zhao et al., 2013). Therefore, the Hg emissions from coal use are estimated based  
124 on the above-mentioned source categories, e.g., power plants, industrial boilers, residential coal stoves,  
125 and iron & steel production (most emissions of which come from coal use). For cement production,  
126 Hg emissions result both from coal combustion and non-combustion processes, and a new method is  
127 developed to differentiate the two parts, as described in Section 2.2.

128 In general, annual emissions of total Hg and the three Hg species are calculated using Eq. (1) and  
129 (2), respectively, for a given province  $i$  and a given year  $t$ :

130 
$$E_{i,t} = \sum_m \sum_n AL_{m,n,i,t} \times EF_{m,n,i,t} \quad (1)$$

131 
$$E_{i,t,s} = \sum_m \sum_n AL_{m,n,i,t} \times EF_{m,n,i,t} \times f_{m,n} \quad (2)$$

132 where  $E$  is the Hg emission;  $AL$  is the activity levels (fuel consumption or industrial production),  $EF$   
 133 is the combined emission factor (emissions per unit of activity level);  $f$  is the mass fraction of a given  
 134 Hg species ( $Hg^0$ ,  $Hg^{2+}$  or  $Hg^p$ ); and  $i$ ,  $t$ ,  $m$ ,  $n$  and  $s$  represent province, year, emission source type,  
 135 technology of manufacturing and emission control, and Hg species.

136 For coal combustion, Eq. (1) can be further revised to Eq. (3) with detailed combustor and fuel  
 137 information:

138 
$$E_{i,t} = \sum_m \sum_n AL_{m,n,i,t} \times HgC_{i,t} \times R_{m,n} \times (1 - \eta_{m,n,t}) \quad (3)$$

139 where  $HgC$  is the Hg content of coal by province;  $R$  is the mass fraction of Hg released from the fuel;  
 140 and  $\eta$  is Hg removal efficiency of air pollution control devices.

141 Due to inadequate information, emissions from ASGM are not calculated based on the emission  
 142 factors and activity levels. ASGM was officially prohibited in the 1990s, although it may still occur  
 143 illegally in some areas because of the huge economic profits. Telmer and Veiga (2009) estimated the  
 144 Hg release from ASGM in 2008 based on available data on Hg and gold exports and imports, and the  
 145 results are widely accepted (AMAP/UNEP, 2013). Muntean et al. (2014) developed a new method to  
 146 estimate historical trends in ASGM activity, based on the market demand for gold and the relatively  
 147 accurate data available on large-scale gold production. They found little inter-annual variation after  
 148 2005 for China. In this work, therefore, the results by Telmer and Veiga (2009) are directly used for  
 149 2005-2012.

150 Activity levels for 2005-2012 are compiled annually by sector from various data sources.  
 151 Multiple-year fossil fuel consumption and industrial production at the provincial level are obtained

152 from Chinese official energy (NBS, 2013a) and industrial economic statistics (NBS, 2013b),  
153 respectively. The coal consumption in CEM and ISP is calculated following the methods of Zhao et al.  
154 (2011; 2012), and the coal consumption by OIB is estimated by subtracting the fuel consumed by  
155 CEM, ISP, and HB from that by IND (Zhao et al., 2012). The annual biofuel use until 2008 is taken  
156 from official statistics (NBS, 2013a); NBS stopped reporting the data in that year, so estimates for  
157 subsequent years are taken from unpublished data of the Ministry of Agriculture (C Chen et al., 2013).  
158 The biomass combusted in open fields is calculated as a product of grain production, waste-to-grain  
159 ratio, and the percentage of residual material burned in the field, as described in Zhao et al. (2011;  
160 2012). The burned urban municipal waste is taken from official statistics (NBS, 2013c), and that in  
161 rural areas is calculated as a product of rural population, the average waste per capita, and the  
162 estimated ratios of waste that is burned (Yao et al., 2009).

163 The Hg emission factors, speciation, and the time-series trends due to improved controls will be  
164 described by sector in Section 3.

## 165 **2.2 Improved methods for estimating emissions from particular sources**

166 The methods of emission estimation for certain sources are improved to better understand the  
167 effectiveness of ongoing pollution control measures in China. Those sources include thermal power  
168 generation, cement and steel production, and nonferrous metal smelting, emissions of which were  
169 estimated in previous studies with uniform, time-independent emission factors averaged at the sector  
170 level.

171 For power plants, detailed information related to emission estimation are compiled at the  
172 generating unit-level, including coal consumption, combustion technology, fuel quality, and the time  
173 and type of emission control technologies applied, based on an updated Chinese power plant database

174 developed by the authors (Zhao et al., 2008). Hg emissions of each plant are then calculated  
175 plant-by-plant based on the unit-specific information using Eq. (3).

176 With improved data on kiln technologies and emission control devices (Lei et al., 2011; Zhao et  
177 al., 2013), their penetrations into the cement industry for a range of years are derived. Hg emission  
178 factors by emission control type, based on domestic measurements, are accordingly applied to  
179 generate the inter-annual trends in emissions. Besides total emissions of the sector, Equation (3) is  
180 used to separately estimate the emissions from coal combustion in cement industry. For nonferrous  
181 metal smelting, similarly, the penetrations of different manufacturing technologies for typical years  
182 (2005, 2007, and 2010) are obtained from a plant-by-plant database developed by Tsinghua  
183 University (Wu et al., 2012), and penetrations for other years have to be interpolated due to lack of  
184 further information. The inter-annual trends of emissions can then be estimated by combining the  
185 penetration and emission factors by technology.

186 For iron & steel production, Hg emissions come mainly from coal-combustion processes  
187 including coking, sintering, and pig-iron production. In recent years, implementation of national  
188 energy-saving and pollution-control policies led to improved energy efficiency and enhanced use of  
189 emission control devices of those processes (Zhao et al., 2013). The updated information is integrated  
190 into Eq. (3) to estimate the Hg emissions for the sector by process and year. In particular, the coal  
191 consumption by process is calculated based on the amount of coal combusted by the whole sector and  
192 the energy efficiency by process (expressed as kg coal-equivalent/t-steel) reported in official statistics.

### 193 **2.3 Uncertainty analysis**

194 The uncertainties of Hg emissions, including by different species, are quantified by sector and  
195 year using a Monte-Carlo framework developed by Zhao et al. (2011). Probability distributions are  
196 estimated for all input parameters, and 10,000 simulations are then performed to estimate the

197 uncertainties of emissions and to identify the crucial parameters that significantly contribute to the  
198 uncertainties for different source types.

199 In most cases, the uncertainties of activity levels (including penetration rates of different  
200 technologies by sector) are determined following our previous work (Zhao et al., 2011; 2013).  
201 Generally, normal distributions are assumed for all the fuel consumption and industrial and  
202 agricultural production, with coefficients of variation (CV, the standard deviation divided by the  
203 mean) set at 5%, 10%, and 20% for power, industry, and residential & commercial sectors,  
204 respectively. A comprehensive analysis of uncertainties of Hg emission factors was conducted by  
205 sector and species, with domestic field measurements thoroughly evaluated. For parameters with  
206 adequate measurement data, the Kolmogorov-Smirnov test for the goodness-of-fit ( $p=0.05$ ) is applied  
207 and, if the test is passed, bootstrap simulation is conducted to determine the probability distribution  
208 (Frey and Zheng, 2002; Zhao et al., 2010; 2011). For parameters that fail to pass the goodness-of-fit  
209 test or those with limited observational data, probability distributions must be assumed based on  
210 previous work (e.g., Wu et al., 2010) and/or the authors' judgments. Details about the emission factor  
211 uncertainties by sector will be discussed in Section 3.

212 For ASGM, in which emissions were not calculated but taken directly from Telmer and Veiga  
213 (2009) as described in section 2.2, the uncertainties are assumed at  $\pm 67\%$  according to expert  
214 judgment (AMAP/UNEP, 2013). Muntean et al. (2014) compared the ASGM emissions estimated  
215 from varied methods and data sources (AGC, 2010; Telmer and Veiga, 2009), and the differences are  
216 within the uncertainty range assumed in this work.

## 217 **2.4 Emission projections to 2030**

218 Three scenarios are devised to project China's atmospheric Hg emissions in 2015, 2020, and  
219 2030. Scenario 0 (S0) is the most conservative case, in which the national policy of energy saving and

220 air pollution control will not change in practice after 2012. This does not imply, however, that the  
221 penetration levels of advanced technologies and emission control devices in specific sectors will  
222 necessarily be the same as in 2012. For example, current policies for the power sector will  
223 undoubtedly raise the use of FGD and SCR systems, and that for cement will increase the share of  
224 precalciner kilns with FF systems (i.e., this share would reach 100% in 2030, compared to 88% in  
225 2012). While keeping the control strategy the same as in S0, Scenario 1 (S1) integrates the national  
226 energy policy commitments that have been announced (e.g., the plans to reduce fossil energy use and  
227 to reduce greenhouse gas emissions) and thus illustrates the benefits of enhanced energy saving on Hg  
228 emissions. The activity-level data for S0 and S1 are taken respectively from the Current Policy  
229 Scenario (CPS) and New Policy Scenario (NPS) of our previous work (Zhao et al., 2014), which are  
230 based mainly on projections by IEA (2012), with revisions in specific sectors including power and  
231 transportation. For sources that are not mentioned in Zhao et al. (2014), specific working reports are  
232 consulted. For example, the burned ratio of urban municipal solid waste is assumed to reach 50% in  
233 2030, according to CAUES (2013). Scenario 2 (S2) shares the same activity level trends as S1 but  
234 includes more stringent emission controls, mainly for industrial sources. Those measures include use  
235 of advanced control devices specifically for Hg removal in new power plants, use of FGD systems in  
236 new industrial and heating boilers, use of SCR in new cement precalciner kilns starting in 2020,  
237 greater penetration of electric furnaces in steel smelting (resulting in less pig-iron production and  
238 thereby less coal combustion), and greater penetration of advanced manufacturing technologies, with  
239 lower Hg emission factors, in nonferrous metal smelting. The detailed control benefits of those  
240 technologies on Hg emissions are described in the next section.

241

## 242 **3 EVOLUTION OF EMISSION FACTORS**

### 243 **3.1 Evolution of emission factors for key sectors, including key assumptions and uncertainties**

244 The improvement of emission factors result mainly from two sources: (1) new and better data  
245 through domestic measurements for key sectors; and (2) better understanding of penetration levels of  
246 manufacturing and control technologies for different sources during 2005-2012. Those improvements  
247 provide more accurate emission factors, with clearer inter-annual trends by sector, as shown in Figure  
248 1. Through comprehensive review of the literature, a database for Hg emission factors (and related  
249 parameters) by sector is established for China, with the uncertainty for each emission factor or  
250 parameter analyzed and presented as a probability distribution function (PDF), as summarized in  
251 Table 1.

#### 252 **Power plants**

253 As Eq. (3) indicates, the integrated Hg emission factor for power plants, expressed in metric tons  
254 (t) of Hg emissions per million metric tons (Mt) coal combusted, is calculated as the product of the  
255 Hg content of coal, the release rate of the specific combustion facility, and the difference of one and  
256 the Hg removal efficiency of a specific air pollution control device (APCD).

257 The Hg content of coal in China has been addressed in a series of studies (Wang et al., 2000;  
258 Huang and Yang, 2002; Feng et al., 2002; USGS, 2004; Zheng et al., 2006; Zhang et al., 2012a), and  
259 the method of Wu et al. (2010) is followed in the current work to determine the values and  
260 uncertainties by province. The percentages of Hg content by province are estimated based on  
261 available measurement data and a conservative assumption of a lognormal distribution is applied as  
262 the PDF, with relatively long tails for the distributions in most provinces. Regarding the release rates,  
263 the values for pulverized combustion (PC), circulating fluidized bed (CFB), and grate boiler systems

264 reach 98.7%, 98.4%, and 95.9%, respectively, reflecting that most Hg in coal is emitted into the flue  
265 gas due to the high combustion temperature (see details in Table S1 in the Supplement). As currently  
266 available measurements are insufficient for data fitting to determine the uncertainties, triangular  
267 distributions are assumed for the parameter, with the lowest and highest measurement values taken as  
268 the 10<sup>th</sup> and 90<sup>th</sup> percentile of each distribution, respectively.

269 Deployment of advanced APCDs in the coal-fired power sector has increased since 2005. The  
270 penetration levels of FGD and SCR systems, for example, reached 90% and 27%, respectively, in  
271 2012. These technologies demonstrably result in lower Hg emission factors and thereby ancillary  
272 benefits in Hg removal (Wang et al., 2012). The removal efficiencies of major types of APCDs,  
273 including ESP, FF, joint ESP and FGD (ESP+FGD), and joint SCR, ESP, and FGD  
274 (SCR+ESP+FGD), are analyzed using the most recent field measurements at China's power plants  
275 (see details in Table S2 in the Supplement). As shown in Figure 2, SCR+ESP+FGD systems have the  
276 highest Hg removal efficiency, at 76.6%, followed by FF at 56.1% and ESP+FGD at 53.8%. Large  
277 variations of Hg removal efficiencies of APCDs are indicated by different studies, and the values  
278 estimated and applied in this work are relatively conservative, particularly for ESP+FGD, which is  
279 currently the dominant APCD configuration in China's power sector. In addition, the removal  
280 efficiencies are much lower than those in developed countries like the U.S. and Japan. Two reasons  
281 could be a large difference in coal qualities between the countries and the poorer operational  
282 conditions of APCDs in China (Li, 2011; Zhi et al., 2013). For other dust collectors including wet  
283 scrubbers (WET) and cyclones (CYC), limited domestic information from field tests (e.g., Huang et  
284 al., 2004) leads to higher removal efficiencies than previous inventories (Streets et al., 2005; Wu et al.,  
285 2006). We believe these values do not significantly raise the uncertainty because the capacity share of  
286 units with either WET or CYC is small, i.e., roughly 2% in 2010.

287        Regarding the prospects for further improvement of Hg emission control in the future,  
288 newly-built power units are assumed to apply powdered activated carbon (PAC) injection technology  
289 (Srivastava et al., 2006; Cui et al., 2011) or modified catalytic oxidation of elemental Hg (Guo et al.,  
290 2011; Yan et al., 2011) in S2, and the average Hg removal efficiencies of those technologies are  
291 expected to reach 90%. The PDFs of removal efficiencies by device are estimated following the  
292 description in Section 2.3. In most cases, the PDFs are assumed to be Weibull distributions due to  
293 insufficient data samples. For ESP, however, the data from currently available measurements pass the  
294 statistical test, and bootstrap simulation is thus conducted to determine a normal PDF, as shown in  
295 Figure S3(a) in the Supplement.

296        Due mainly to the sharply growing use of APCDs, the average Hg emission factor for power  
297 plants is estimated to have decreased from 0.13 g/t-coal in 2005 to 0.08 in 2012, as shown in Figure  
298 1(a). With PAC injection applied in the future under S2, the average emission factor would further  
299 decline to 0.05 g/t-coal in 2030.

### 300 **Iron & steel production**

301        In previous studies, a uniform emission factor of 0.04 g/t-steel has generally been applied for  
302 iron & steel production, with little consideration of improving production technologies (Streets et al.,  
303 2005; Wu et al., 2006). In this work, as described in Section 2.2, the latest information on APCD  
304 penetration trends and removal efficiencies is combined, Hg emissions are calculated separately for  
305 each coal-consuming process using Eq. (3), and these are then aggregated to the sector level. The Hg  
306 release ratios of coking and pig-iron production are estimated at 63% and 84%, respectively (Wang et  
307 al., 2000; Hong et al., 2004), with uniform distributions conservatively assumed due to a lack of  
308 updated measurements. Without specific further information, the removal efficiencies and PDFs for  
309 the iron & steel industry are assumed to be the same as those for the power sector. This assumption is

310 expected to result in a possible underestimate of emissions for the sector, because the APCD  
311 operations may not be as thorough as those at power plants, given the greater regulatory oversight of  
312 the latter in recent years. Although this possible underestimate could be partly quantified by  
313 uncertainty analysis, more investigation of the APCD benefits on Hg removal for the iron & steel  
314 sector is needed first (as is also the case with other non-power industrial sectors).

315 Driven by the increased penetration of advanced manufacturing and emission control  
316 technologies, in particular the growth of mechanized coking ovens, the emission factor for iron &  
317 steel production is estimated to have declined from 0.071 to 0.039 g/t-steel from 2005 to 2012,  
318 indicating that the application of 0.04 g/t-steel in earlier studies might have underestimated the  
319 emissions for this sector in previous years (Figure 1(b)). Regarding the future projection, the ratio of  
320 pig iron to steel is assumed to decrease from 92% in 2012 to 80% in 2030 in S2, due to expanding use  
321 of electric arc furnaces that use more waste-steel inputs instead of more energy-intensive inputs  
322 including pig iron (Wang et al., 2007; Zhao et al., 2012). The emission factor would thus decline  
323 further to 0.035 g/t-steel.

#### 324 **Non-ferrous metal smelting**

325 Although the non-ferrous metal industry, including smelting of Pb, Zn, and Cu, is one of the  
326 main sources of Hg emissions (Li et al., 2010; Wu et al., 2012), available emission factors from field  
327 tests are still limited, given the many and complex factors that determine emission levels (e.g., the Hg  
328 concentration in ore concentrate, smelting technology, and the penetration of acid plants and APCDs).  
329 Due to these limited data, a process-based methodology is developed to estimate the emission factors  
330 for various kinds of smelters employed in China, as shown in Table S3 in the Supplement.  
331 Information on all of the processes and their corresponding emission factors are obtained from direct  
332 field measurements (Feng et al., 2004; G. Li et al., 2009; Li et al., 2010; Wang et al., 2010; Zhang et

333 al., 2012b) or field-based calculations (Wu et al. 2012). Given the very small sample sizes, uniform  
334 distributions have to be assumed for most processes, with the lowest and highest measurement values  
335 subjectively taken as the 10<sup>th</sup> and 90<sup>th</sup> percentile of each distribution, respectively. This conservative  
336 assumption provides relatively large variation of emission factors, indicating big uncertainties for  
337 them due to insufficient domestic field measurements. Notably, the oxygen-pressure leaching process  
338 for Zinc smelting has not been included in the table, because it does not include the process of  
339 high-temperature calcination and thus little mercury is released to the atmosphere.

340 Based on a plant-by-plant database (Wu et al., 2012) and a list of small smelters that have been  
341 shut down since 2010, the penetrations of various kinds of smelters are calculated by year and  
342 non-ferrous metal type, and the inter-annual trends of emission factors are then analyzed. As shown in  
343 Figure 1(d)-(f), the national average EFs for Zn, Pb, and Cu smelting are estimated to have dropped  
344 from 15.5, 16.7, and 1.7 g/t-product in 2005 to 13.3, 4.7, and 0.2 g/t in 2012, respectively. In the  
345 future projection of S2, the EFs are projected based on the assumption that the most advanced  
346 technologies will be required at all new smelters. The EFs for Zn and Pb are thus estimated to decline  
347 further to 9.1 and 2.2 g/t-product in 2030, respectively.

#### 348 **Cement production**

349 A series of studies have been conducted to measure the Hg emission levels of cement production  
350 (Li, 2011; Zhang, 2007). Based on the available data from those field tests, the emission factors are  
351 estimated at 0.008, 0.052, and 0.120 g/t-product for cement kilns with FF, ESP, and WET dust  
352 collectors, respectively. The data sample for FF passes the statistical test and bootstrap simulation is  
353 applied to determine its PDF as a Weibull distribution, as shown in Figure S1(b) in the Supplement.  
354 For other dust collectors, however, the current data are too limited and uniform distributions are used,

355 with the lowest and highest measurement values taken as the 10<sup>th</sup> and 90<sup>th</sup> percentile of each  
356 distribution, respectively.

357 Combining the inter-annual trends of APCD penetration for the sector (Lei et al., 2011; Zhao et  
358 al., 2013), the national average emission factor is estimated to have declined from 0.06 in 2005 to  
359 0.018 g/t in 2012 (Figure 1(c)), resulting mainly from the increased use of precalciner kilns with FF.  
360 For the future, all kilns other than precalciners are expected to be closed by 2020 in S1 and S2, and by  
361 2030 in S0. In addition, SCR systems are assumed to be deployed at all precalciner kilns in S2 (Zhao  
362 et al., 2014). These improvements would lead to reductions in the sector-average EFs to 0.013, 0.012,  
363 and 0.008 g/t-product in S0, S1, and S2, respectively, in 2030. Regarding the emissions from coal  
364 combustion in cement production, the Hg removal efficiencies for various APCDs are applied to  
365 generate the emission factors, and the national average value is estimated to have declined from 0.11  
366 to 0.08 g/t-coal during 2005-2012. While no significant abatement is found for S0 and S1 after 2010,  
367 the emission factor would further decrease to 0.04 g/t-coal in S2 by 2030, attributed to the greater use  
368 of SCR in the scenario.

### 369 **Other industrial sources**

370 The emission factors of industrial and heating boilers are estimated using Eq. (3). The Hg release  
371 ratios for grate boilers and CFB are estimated at 76% and 91% based on limited domestic  
372 measurements (Wang et al., 2000; Tang et al., 2004), and are lower than those of power plants.  
373 Uniform distributions are assumed to quantify the uncertainty of the parameter. WET and CYC are  
374 the dominant types of dust collectors for boilers and their removal efficiencies with PDF are assumed  
375 to be the same as those for power plants. For the future under S2, FGD is assumed to be deployed at  
376 all new boilers, leading to a larger fraction of Hg removal.

377 Production of polyvinyl chloride polymer (PVC) is a significant contributor to Hg emissions due  
378 to wide use of mercuric chloride catalyst in acetylene-making processes. The emission factor is  
379 calculated as the product of the Hg content in PVC and its atmospheric release ratio during the  
380 production process. The Hg content in PVC is estimated to range from 0.12 to 0.20 kg Hg/t-PVC,  
381 based on investigation by Hao et al. (2005), and the release ratio to be 1%, according to THU (2009).  
382 For other processes including Hg mining, production of batteries and fluorescent lamps, large-scale  
383 gold production, and oil and gas combustion, the emission factors from AP-42 (USEPA, 2002a) and  
384 previous inventory work (Streets et al., 2005) are used due to lack of updated information from  
385 domestic measurements. Given the big uncertainties for those emission factors, lognormal  
386 distributions are assumed for them with the CV conservatively set at 100%, as suggested by Bond et  
387 al. (2004).

#### 388 **Residential sources**

389 For residential coal consumption, the determination of Hg emission factors is similar to that of  
390 industrial boilers. Biomass combustion takes account of crop residues (used as biofuel in households  
391 and as waste burned in open fields) and fuel wood (used in households). Domestic information and  
392 field measurements are adopted from Huang et al. (2011) and Zhang et al. (2013) to estimate the  
393 emission factors, and uniform distributions are assumed reflecting the relatively high uncertainty.  
394 Based on the domestic dataset, the average EFs for combustion of crop residues (16.7 ng/g) and fuel  
395 wood (12.3 ng/g) calculated in this work are lower than the values adopted in previous literature (e.g.,  
396 37 ng/g for crop residues and 20 ng/g for fuel wood, Streets et al., 2005).

397 Hg emissions from solid waste incineration (SWI) are estimated separately for municipal solid  
398 waste incineration (MSWI) and rural household waste incineration (RHWI), due to different mercury  
399 content levels and burning techniques. For MSWI, an emission factor of 0.22 g/t with Weibull

400 distribution is estimated, with bootstrap simulation based on domestic field tests by L Chen et al.  
401 (2013) and Hu et al. (2012) (Figure S1(c) in the Supplement). The emission factor for RHWI is  
402 estimated as the product of Hg content and the atmospheric release ratio, which are obtained from Hu  
403 et al. (2012).

### 404 **3.2 Speciation of Hg with probability distribution functions**

405 The speciation of Hg plays a crucial role in its atmospheric fate and transport, and chemical  
406 cycling. The fate of Hg released to atmosphere varies by species ( $\text{Hg}^0$ ,  $\text{Hg}^{2+}$ , and  $\text{Hg}^{\text{p}}$ ), which in turn  
407 are determined by fuel quality and the removal mechanisms of APCDs, thereby varying significantly  
408 by emission source. A thorough review of existing studies is conducted to compile a database of Hg  
409 speciation by sector, and to provide the mass fractions of the three main chemical forms (see details in  
410 Table S4 in the Supplement). In general, the emission sources that determine Hg speciation can be  
411 divided into three categories, according to the nature of APCD deployment and data availability. First  
412 are those sources whose emission factors can be calculated based on the removal efficiencies of  
413 different APCD (e.g., CPP, CEM, ISP, OIB and RC), in which case the mass fractions are estimated  
414 based on results from field measurements by type of APCD. Second are sources with insufficient  
415 measurement samples to determine emission factors by APCD, in which case the average values of  
416 available field test results are calculated and directly applied as the mass fractions of the three species  
417 for the sector (e.g., NMS, BIO and SWI). Third are sources for which very little domestic information  
418 about speciation can be found, in which case results from global studies (Pacyna and Pacyna, 2002)  
419 have to be used, with little update to previous inventories (Streets et al., 2005). Those sources mainly  
420 include industrial processes like artisanal gold production, Hg mining, and battery and fluorescent  
421 lamp production.

422 As shown in Table S4, the speciation of total Hg varies considerably by different types of APCD  
423 configurations. For example, the  $\text{Hg}^0$  mass fraction averaged over all estimates in the literature is 83%  
424 for ESP+FGD, attributed to the relatively strong removal effects of both ESP and FGD on  $\text{Hg}^{2+}$  and  
425  $\text{Hg}^p$ . Inclusion of SCR leads to significant increase in the  $\text{Hg}^{2+}$  fraction, resulting mainly from the  
426 conversion of  $\text{Hg}^0$  to  $\text{Hg}^{2+}$  by the SCR process (Wang et al., 2010b). In general, oxidation of  $\text{Hg}^0$   
427 leads to higher removal of Hg because  $\text{Hg}^{2+}$  is more liable to be adsorbed in FGD scrubber solution,  
428 and use of advanced dust collectors leads to lower  $\text{Hg}^p$  as most of it can be captured on particles.

429 For mass fraction data that pass the Kolmogorov-Smirnov test, bootstrap simulation is applied to  
430 determine a PDF, e.g., the mass fractions of  $\text{Hg}^{2+}$  for ESP, ESP+FGD and SCR+ESP+FGD (Figure  
431 S1(d)-(f) in the Supplement). Otherwise, triangular or uniform distributions are applied. The PDFs for  
432 Hg speciation are summarized in Table 2.

433

## 434 **4 RESULTS AND DISCUSSION**

### 435 **4.1 Historical trends in mercury emissions to the atmosphere**

436 The total national emissions of anthropogenic Hg are estimated to have increased from 679.0 t in  
437 2005 to 749.8 t in 2012, with a peak of 770.6 t in 2011, as shown in Figure 3. The annual growth rate  
438 of emissions averaged 1.4% during 2005-2012, much lower than that of China's energy consumption  
439 (7.6%) or the economy (>10%). The result reflects effective constraints on Hg emissions since 2005,  
440 compared to relatively fast growth in early 2000s (e.g., 8% annual growth of Hg emissions from 2000  
441 to 2003 suggested by Wu et al. (2006)). This national trend, however, is currently difficult to confirm  
442 fully with field observations, given the lack of long-term monitoring data for atmospheric ambient Hg  
443 in either polluted cities or background regions. Limited inter-annual results for one background area

444 (Changbai Mountain in northeastern China) show reduced Hg levels (Wan et al., 2009; Fu et al.,  
445 2012b), but those differences are believed to result from changes in sampling location rather than  
446 emissions (personal communication with X. Fu of the Institute of Geochemistry, Chinese Academy of  
447 Sciences, 2014). For speciation of Hg emissions, clear changes are found for different sectors. For  
448 example, the fraction of  $\text{Hg}^0$  to total Hg for power generation is estimated to increase from 59% to  
449 75% during 2005-2012, due to increased use of FGD systems; while that for cement and iron & steel  
450 production decrease from 44% to 33% and 43% to 30%, respectively, due to increased use of fabric  
451 filters. The varied speciation of emissions from different sectors compensates each other, leading to  
452 relatively stable speciation of total anthropogenic Hg emissions for recent years (around 55%, 39%,  
453 and 6% for  $\text{Hg}^0$ ,  $\text{Hg}^{2+}$ , and  $\text{Hg}^p$ , respectively).

454 The annual emissions by source category are summarized in Table 3. Coal combustion, gold  
455 mining, and nonferrous metal smelting are the largest sources of anthropogenic Hg, accounting  
456 together for 85% of national total emissions. The share of coal combustion (from the power sector,  
457 industrial and heating boilers, cement kilns, residential stoves, and iron & steel production, in  
458 declining order) to total national emissions is estimated to have increased from 43% in 2005 to 49%  
459 in 2012. This is mainly due to relatively constant emission levels of gold mining and nonferrous metal  
460 sectors during the same period, resulting from penetration of newer and more advanced mining and  
461 manufacturing technologies. Emissions of  $\text{Hg}^0$ ,  $\text{Hg}^{2+}$  and  $\text{Hg}^p$  are summarized by sector in Table  
462 S5-S7 of the Supplement. For  $\text{Hg}^0$  and  $\text{Hg}^{2+}$ , the three biggest sources are the same as those for total  
463 Hg emissions, i.e., coal combustion, gold mining, and nonferrous metal smelting. For  $\text{Hg}^p$ , coal  
464 combustion plays a dominant role, with the share ranging 78%-84% for various years, as very little  
465  $\text{Hg}^p$  emissions are estimated from gold mining, zinc smelting, and lead smelting.

466 Provincial emissions, including inter-annual variations, are assessed and illustrated in Figure 4.  
467 Because of uncertainties about both emission levels and spatial distribution, Hg emissions from  
468 ASGM are omitted from the provincial analysis. While coal combustion is identified as the biggest  
469 source of atmospheric Hg in most provinces, relatively high emissions from non-combustion sources  
470 are estimated for several provinces including Hunan, Yunnan, Henan, Guangxi, Anhui, and Shaanxi,  
471 resulting mainly from the large production of Zn and/or Pb in those regions. Clear differences in  
472 emission trends from 2005 to 2012 are found by region. In contrast to most provinces that have seen  
473 increasing emissions, the three regions with the highest densities of population, economic activity,  
474 and other pollution show declining estimated emissions, i.e., the Jing-Jin-Ji region (JJJ, including  
475 Beijing, Tianjin and Hebei), the Yangtze River Delta region (YRD, including Shanghai, Jiangsu and  
476 Zhejiang), and the Pearl River Delta region (PRD, including Guangdong). The collective share of  
477 total Hg emissions of the 7 provinces in these regions is estimated to have declined from 24% in 2005  
478 to 19% in 2012, which is similar to trends in criteria air pollutants (Zhao et al., 2013). On one hand,  
479 this regional deviation indicates slower growth in heavily polluting industry and the progress of  
480 emission controls in highly developed regions. On the other hand, it indicates that China's air  
481 pollution challenges have been expanding to less developed interior provinces, which are  
482 experiencing rapid urbanization, accelerated economic development, and fast growth of pollution  
483 sources.

484 To be applicable to simulation of atmospheric transport and chemistry, annual Hg emissions at  
485 the provincial level are allocated to a  $0.25^{\circ} \times 0.25^{\circ}$  grid system, applying the methods described in  
486 Zhao et al. (2012). Note the emissions from production of coal-fired power, cement, and iron & steel  
487 are allocated at the unit or plant level (e.g., Figure S2(a) in the Supplement for coal-fired power

488 plants). Shown in Figure S2(b)-(d) are the gridded emissions of China's anthropogenic  $\text{Hg}^0$ ,  $\text{Hg}^{2+}$  and  
489  $\text{Hg}^p$ , respectively.

#### 490 **4.2 Implication of emission controls on national Hg emissions**

491 China's anthropogenic Hg emissions have not increased as rapidly compared to the country's  
492 economic growth, reflecting the success of national strategies in broader emission control. While  
493 collectively causing this national trend, emission trends by sector have varied greatly due to different  
494 driving factors and uneven control policies. More detailed analysis is needed to disentangle the  
495 sources contributing most to the Hg emission trends. Particularly high uncertainty undermines  
496 estimation of emissions from ASGM, due to scarcity of input data and information, and its annual  
497 emission level is assumed unchanged over time in this work. Although recognized as the largest  
498 contributor of the individual sources to total Hg emissions (Table 3), ASGM must unfortunately be  
499 omitted here as a source type affecting the national emission trend due to these data constraints.

500 We divided the remaining anthropogenic sources into three categories, as indicated in Figure 5(a).  
501 The first category includes sources for which uniform and unchanged emission factors are applied  
502 over time (i.e., LGM, BIO, SWI, and OMP). The inter-annual variability of Hg emissions from those  
503 sources are thereby only affected by the changes of activity levels, and the annual emissions for  
504 Category 1 sectors have continued to increase, from 80.3 t in 2005 to 109.8 t in 2012. Due to their  
505 relatively small fraction of total emissions (<15%), however, the Category 1 sectors have little  
506 influence on the trend of the national total, which shows much slower growth and even reduced  
507 emissions in a few years, as shown in Figure 5(a). Category 2 consists of industrial fuel combustion  
508 (HB and OIB), and residential use (RC and ROG), those for which emission factors are  
509 region-dependent and show little inter-annual variation due to very limited implementation of  
510 pollution control measures. The Hg emission trend of these sources therefore depends mainly on the

511 intensive coal use in recent years, and estimated emissions in 2012 are 47% higher than those of 2005.  
512 Category 3 includes CPP, CEM, ISP, and NMS. Although the activity levels (i.e., coal consumption  
513 and industrial production) increased in these sources at similar rates as the sectors of Categories 1 and  
514 2, the Hg emission trends of Category 3 sectors are dominated by the combined effects of improved  
515 manufacturing technologies and increased use of APCDs to control criteria air pollutants. The  
516 emissions of these sectors are estimated to have peaked at 362 t in 2007, and then to have declined to  
517 313 t in 2012, largely offsetting the increase in emissions from Categories 1 and 2 and playing a  
518 crucial role in constraining total national emissions.

519 Figure 5(b) compares the trends of activity levels and Hg emissions for Category 3 sectors from  
520 2005 to 2012. During the period, coal consumption from production of coal-fired power, cement, steel,  
521 and nonferrous metals increased by 70%, 107%, 158%, and 104%, respectively. A leveling of  
522 industrial production is found in 2008, attributed to production constraints imposed for the Beijing  
523 Olympics and to the economic recession at the end of 2008. However, economic activities increased  
524 sharply again under a major economic stimulus policy responding to the recession, and energy and  
525 industrial production continued to grow swiftly in the following years. Despite the fast growth of  
526 activity levels, however, the Hg emissions from the four sectors were clearly constrained, to varying  
527 degrees: those from CEM decreased by 38%, those from CPP and NMS in 2012 returned to the levels  
528 of 2005, and only those from ISP increased, by 44%, though still far less than growth of steel  
529 production. As described in Section 3, the reduced emission factors through the period are the main  
530 reasons for the emission abatement, attributed to the replacement of old and small plants or kilns with  
531 larger ones with high combustion efficiencies and advanced control technologies. The increased  
532 penetrations of FGD and SCR systems in CPP, precalciner kilns with FF in CEM, mechanized coking  
533 ovens with ESP in ISP, and improved manufacturing technologies in NMS have lead to great ancillary

534 benefits of atmospheric Hg emission abatement. As indicated in Figure S3 in the Supplement, the  
535 emission controls are estimated to have cut 100, 93, 30, and 76 t of Hg emissions in 2012 for CPP,  
536 CEM, ISP and NMS, respectively, compared to a hypothetical case in which no progress of emission  
537 control is assumed for the four sectors since 2005. Without the controls, the Hg emissions of those  
538 sectors in 2012 would have exceeded 600 t, almost double the current estimate. This shows that  
539 China's pollution controls in power and key industrial sectors have slowed national Hg emissions, and  
540 that energy consumption and industrial production are poor proxies for Hg emissions.

#### 541 **4.3 Evaluation of the estimated emissions against other studies**

542 There are several global inventories that include data for China, including those by the United  
543 Nations Environment Programme (AMAP/UNEP, 2008; 2013; Pacyna et al., 2010), International  
544 Institute for Applied System Analysis (IIASA, Rafaj et al., 2013), Emission Database for Global  
545 Atmospheric Research (EDGAR, Muntean et al., 2014), and Peking University (Y Chen et al., 2013).  
546 The trends in China's Hg emissions estimated in the current work is difficult to compare directly to  
547 those studies for two reasons: 1) limited studies have been conducted of China's national total Hg  
548 emissions for the most recent years, a period with large changes in emission controls across the  
549 country; and 2) the sectors and sources of anthropogenic Hg emissions are not defined similarly in  
550 different inventories. For earlier years, Wu et al. (2006) estimated China's anthropogenic Hg  
551 emissions increased from 552 in 1995 to 696 t in 2003, with a higher annual growth rate (2.9%) than  
552 this work for 2005-2012 (1.4%). The results of speciation analysis are similar between Wu et al.  
553 (2006) and this work, with slightly larger mass fraction of Hg<sup>p</sup> (12% vs. 6%) but a smaller one of  
554 Hg<sup>2+</sup> (32% vs. 39%) in Wu et al. This is probably due to oxidation of Hg<sup>0</sup> by APCDs and increased  
555 use of advanced dust collectors after 2005.

556 Illustrated in Figure 3 are the estimates of China's anthropogenic Hg emissions for various years  
557 between 2005 and 2012 from different inventories. (Note that estimates by Y Chen et al. (2013) are  
558 not shown because that study included only combustion sources, not all anthropogenic sources.) Our  
559 estimates are generally larger than those of global inventories, except for the results of UNEP for  
560 2005 (AMAP/UNEP, 2008). In particular, the estimates for 2005-2008 by Muntean et al. (2014) are  
561 clearly below the lower bounds of 95% confidence intervals (CI) of this work (see Section 4.4 for  
562 details). Our higher estimate is supported by limited top-down studies, e.g., Pan et al. (2007), who  
563 applied an inverse modeling method with four-dimensional variational data assimilation and derived a  
564 larger Hg<sup>0</sup> emission estimate than those from bottom-up methods. Most recent studies evaluated the  
565 annual emissions of China's anthropogenic Hg at 643 t for 2007 (Wang et al., 2014) and 494 t for  
566 2008 (Muntean et al., 2014), i.e., 101 and 248 t smaller than our estimates, respectively. Wang et al.  
567 (2014) and Muntean et al. (2014) further applied their emissions in GEOS-Chem model and the  
568 simulated ambient total Hg or Hg<sup>0</sup> concentrations were generally lower than observation at  
569 background/rural sites across the country, implying a possible underestimate of Hg emissions.

570 To better understand the reasons for the discrepancies of various studies, the emissions from  
571 particular sectors in global inventories and in this work are summarized and compared in Table S8 in  
572 the Supplement. For 2005, the much higher emissions of CPP and the combined HB & OIB sectors in  
573 the UNEP inventory (AMAP/UNEP, 2008; Pacyna et al., 2010) than ours estimates mainly from little  
574 consideration of emission controls and thereby larger emission factors for those sources. For 2010,  
575 however, lower emissions of CPP are estimated in the UNEP inventory (AMAP/UNEP, 2013),  
576 attributed mainly to both higher penetrations and higher Hg removal efficiencies of APCDs compared  
577 to our estimates. The large differences in emissions from HB & OIB and NMS are the main sources  
578 of higher national totals in our inventory than most of the other global inventories. For example,

579 AMAP/UNEP (2013) uses the energy data from the International Energy Agency, which estimates  
580 coal consumption of China's industrial boilers as 110 Mt lower than the official data used here for  
581 2010. FF systems, which are able to capture some Hg emissions, are assumed to be deployed at 25%  
582 of Chinese industrial boilers by AMAP/UNEP (2013), while our data indicates a much lower  
583 penetration. For NMS, AMAP/UNEP (2013) and Muntean et al. (2014) apply activity data from  
584 USGS (2011), which provides lower nonferrous metal production estimates than NBS (2013b).  
585 Muntean et al. (2014) uses emission factors from EMEP/EEA (2009), i.e., 5 g/t-Zn, 0.9 g/t-Pb, and  
586 0.03 g/t-Cu, much lower than our results.

587 Besides the total emissions, several studies have been conducted to analyze the Hg emissions  
588 from certain sectors in China. For coal combustion sources as a whole, Tian et al. (2010) calculated  
589 the Hg emissions at 284 and 306 t for 2005 and 2007, respectively, within 10% of our estimates. Y  
590 Chen et al. (2013) calculated China's Hg emissions from coal combustion at 362 t for 2007, of which  
591 the emissions from CPP were 204 t, much larger than our estimate of 152 t. From a global perspective,  
592 Y Chen et al. (2013) estimated the penetrations of APCD by country using a parameterized function,  
593 and derived relatively low fractions of APCD for the power sector in China. Streets et al. (2009b)  
594 calculated the emissions from CPP at 125 t for 2005, while Tian et al. (2012) estimated that annual  
595 emissions from CPP during 2005-2007 ranged 135-139 t, with little inter-annual variability. Those  
596 estimates are somewhat lower than our results. Although the differences could be attributed to many  
597 factors including discrepancies in details regarding boiler technologies and data sources of Hg content  
598 of coal, the relatively conservative removal efficiencies of APCDs for Hg assessed and applied by us  
599 (as shown in Figure 2) are believed to be the most important reason for the higher estimate of Hg  
600 emissions. Wang et al. (2010c) estimated that Hg emissions from CPP would reach 155 t in 2010,  
601 higher than our results. However, the energy data and penetrations of APCDs (especially FGD) in

602 Wang et al. (2010c) were predictions based on Zhao et al. (2008), as the official statistics for 2010  
603 were unavailable when the study was conducted. The larger annual coal consumption by CPP and  
604 lower penetration of FGDs in the study compared to the official statistics (1735 Mt vs. 1576 Mt, and  
605 70% vs. 86%, respectively) could lead to an overestimate of Hg emissions for the sector.

606 For NMS, previous inventories commonly used constant emission factors, citing lack of detailed  
607 analyses of the trends in manufacturing technology penetration and thereby any ancillary effects on  
608 Hg emissions. Feng et al. (2009) summarized results from previous studies and estimated that the  
609 emission factors of NMS in China for 1995-2003 could reach as high as 6-155 g/t-Zn, 44 g/t-Pb, and  
610 10 g/t-Cu, while Pirrone et al. (2010) adopted 7 g/t-Zn, 3 g/t-Pb, and 5 g/t-Cu for a 2003 emission  
611 estimate for China, based on results from developed countries. If those two sets of EF values are  
612 applied while ignoring possible variation over time, Hg emissions from NPS in 2012 would be 475 t  
613 and 80 t, i.e., 420% larger and 12% lower than this work, respectively. The big gaps between different  
614 estimates, as indicated in Figure 6(a), reveal the importance of better tracking the inter-annual trends  
615 of emission factors for the sector. Based on a detailed survey on individual smelting plants, a more  
616 recent study by Wu et al. (2012) developed a technology-based methodology with consideration of  
617 smelting processes, mercury concentrations in ore concentrates, and mercury removal efficiencies of  
618 APCDs. They calculated that emissions declined from 87 in 2005 to 72 t in 2010, more consistent  
619 with our study than those using constant emission factors.

620 For ISP and CEM, emission factors in previous inventories were mainly obtained from Pacyna  
621 and Pacyna (2002) and Streets et al. (2005), respectively, i.e., 0.04 g/t-product. With these uniform  
622 emission factors adopted, estimated Hg emissions from the two sectors during 2005-2012 would  
623 continue increasing from 15 to 38 and 43 to 88 t, respectively, as shown in Figure 6 (b) and (c). This  
624 ignores the effects of improved manufacturing technologies and increased use of APCDs, and would

625 potentially overestimate emissions, particularly in recent years. For MSWI, the emission factor of 2.8  
626 g/t from UNECE/EMEP (2004) was widely accepted in previous inventories. A series of domestic  
627 field measurements, however, suggested a much smaller value of 0.22 g/t for China (L Chen et al.,  
628 2013; Hu et al. 2012), and lower emissions are estimated in this work (Figure 6(d)). Given the swift  
629 growth of solid wastes in China, more field tests on both municipal and rural solid waste burning  
630 plants are thus imperative to confirm the levels of emission factors and to reduce the uncertainties of  
631 Hg emission estimates for these sources.

#### 632 **4.4 Uncertainties of national emission inventory**

633 The uncertainties of anthropogenic Hg emissions in China for 2005-2012 are quantified using  
634 Monte-Carlo simulation and the results for selected years are summarized in Table 4. In 2010, for  
635 example, the uncertainties of total Hg emissions and those from coal combustion are estimated at  
636 -23%–+51% (95% CI) and -49%–+69%, respectively. Since the annual emissions from ASGM and  
637 associated uncertainties are assumed to be unchanged during the period and are thus comparatively  
638 subjective, the uncertainties of anthropogenic Hg emissions excluding ASGM is further calculated, at  
639 -23%–+61% (95% CI). The uncertainties of the current Hg emission inventory are believed to be  
640 partly responsible for the differences in ambient Hg levels between observations and model  
641 simulations (e.g., a 0-50% difference suggested by Wang et al., 2014). Larger uncertainties are found  
642 for individual Hg species than for total Hg, e.g., -31%–+58%, -32%–+69%, and -51%–+114% (95%  
643 CIs) for Hg<sup>0</sup>, Hg<sup>2+</sup>, and Hg<sup>p</sup> in 2010, respectively (not shown in the table). Among the three aggregate  
644 sectors (CPP, IND, and RES), the uncertainties of IND are relatively small. This does not imply that  
645 the emission characteristics of IND are well understood, however, but rather results from the  
646 aggregation of the uncertainties of all industrial sources. It thus cannot reflect larger uncertainties for  
647 particular IND sources.

648 Figure S4 illustrates the emission estimates and uncertainties by source for different Hg species  
649 in 2010. For all species, BIO, SWI and ROG are the sources with the largest estimated uncertainty  
650 relative to their central estimates (i.e., 95% CIs expressed in percentages). However, particular  
651 industrial sources, including those with less relative uncertainty, are better determinants of the  
652 national Hg emission uncertainty, because of their large fractions of total emissions. Those sources  
653 include CPP for Hg<sup>0</sup>, NMS and GM for Hg<sup>0</sup> and Hg<sup>2+</sup>, and OIB and RC for Hg<sup>p</sup>.

654 Table 5 summarizes the parameters that are important in determining the uncertainties of  
655 emissions according to their contributions to the variance of emissions. In most cases, parameters  
656 related to emission factors contribute most to the uncertainties, including the Hg content of coal in  
657 provinces with large consumption (e.g., Shandong and Henan), emission factors of biomass burning  
658 and particular technologies for nonferrous metal smelting, and the removal efficiencies of dominant  
659 APCDs. The amount of burned coal and biomass are found to be important specifically to the  
660 emission uncertainty of the residential sector. For individual species, the mass fractions of different  
661 species for various APCDs and gold mining are identified as key determinants of uncertainty.

662 It should be noted that no inter-annual variation for those parameters related to emission factors  
663 is assumed for the research period, even if large uncertainty exists for them in a given year. Thus each  
664 individual parameter or emission factor applied for estimation of emission uncertainties for a given  
665 year is statistically correlated with it for another year in the Monte-Carlo simulation framework.  
666 Under this ideal assumption, the uncertainties in emissions for an individual year, whether big or  
667 small, are not associated with the inter-annual trends in emissions.

668 Inclusion of more results from recent measurements of emission factors reduces the uncertainty  
669 of CPP for 2005 estimated here compared to that estimated for 2003 by Wu et al. (2003). It can be  
670 seen from Table 4, however, that the uncertainties of emissions from CPP increased from 2005 to

671 2012. This results mainly from the fast penetration of FGD systems after 2005 and that of SCR after  
672 2010, of which the ancillary effects on Hg control varied significantly among measured plants. In past  
673 years, installed FGD systems were believed to be operated sporadically, in order to save operational  
674 costs, and large discrepancies in estimated SO<sub>2</sub>-removal efficiencies exist across the country (Xu,  
675 2011; Zhao et al., 2013; 2014). The unclear operation of FGD causes a wide range of estimated Hg  
676 removal efficiencies of the systems and thus enhances the uncertainties of the emission estimate, as  
677 FGD usage increases in the sector over the study period. In addition, the Hg removal effects of SCR  
678 are still poorly quantified, and the uncertainties of Hg emissions are further elevated in recent years  
679 because China is currently undertaking NO<sub>x</sub> control largely through expanded use of SCR (Zhao et al.,  
680 2014). As shown in Figure 7, the contribution of Hg removal efficiency of FGD to the variance of  
681 CPP emissions increases from 0% in 2005 to 26% in 2010, and it has been the most important  
682 parameter contributing to the uncertainty of CPP emissions since 2009. In 2012, Hg removal  
683 efficiencies of FGD and SCR are estimated to collectively contribute 37% of the uncertainty of Hg  
684 emissions. The emission uncertainties of given industrial sources increased recently for similar  
685 reasons. The uncertainty of Hg emissions from NMS, for example, increased from -46%–+116% in  
686 2005 to -45%–+169% in 2012. This is attributed mainly to the increased use of electrolytic processes  
687 in Zinc smelting, for which domestic measurements are rare and the emission factor has high  
688 uncertainty. Moreover, the reduced ratios of gold extraction by amalgamation, reported but  
689 unconfirmed, enhance the Hg emission uncertainty of gold mining. In general, therefore, the  
690 uncertainty of Hg emissions is higher in the most recent years and may continue to be so in the near  
691 future. More field tests or investigations of particularly important sectors are needed for better  
692 understanding of the evolution of emission sources and their benefits to Hg control.

#### 693 **4.5 Future emission trends by scenarios**

694 The projected national emissions through 2030 are summarized by sector in Table 6. As shown  
695 in Figure 3 and Table 6, China's anthropogenic Hg emissions are likely to increase slightly in the  
696 future, even with a few new Hg-specific control measures, judged by scenarios S0 and S1. The  
697 emissions in 2030 for the two scenarios are estimated at 869 and 813 t, i.e., 16% and 8% higher than  
698 2012, respectively. The estimated growth in Hg emissions continues to be slower than that of the  
699 economy and energy consumption projected by IEA (2012). This results mainly from the ancillary  
700 benefits of ongoing control policies targeting other pollutants in the country, such as the National  
701 Action Plan for Air Pollution Prevention and Control (Zhao et al., 2014). The results suggest that  
702 projecting China's Hg trajectory based only on economic and/or energy growth would likely lead to  
703 overestimation.

704 Comparing the three scenarios, S2 produces a much larger reduction in Hg emissions over S0  
705 than does S1. This suggests that implementation of Hg-specific controls may offer more effective  
706 emission reduction than relying on the ancillary benefits of energy conservation. In particular, if key  
707 industrial sources including ASGM can be controlled by national regulations (two thirds of such  
708 emissions are assumed to be cut in S2, based on an estimate by Feng et al. (2009)), the national Hg  
709 emissions from 2015 on would be less than those of 2005, and by 2030 would be less than 600 t, 23%  
710 below the 2012 total. For industrial sources other than metallurgy, however, the Hg abatement in S2 is  
711 relatively modest, implying small future ancillary effects on Hg of APCDs due to their nearly  
712 saturated deployment in most sectors. Expanded use of Hg-specific removal devices in sectors such as  
713 power generation and heavy industry is thus essential to further reduce Hg emissions in the future. In  
714 addition, very few effective policies are identified that target residential sources, resulting in elevated

715 emissions for that sector. The RES share of total anthropogenic Hg emissions in S2 is thus projected  
716 to rise from 11% in 2012 to 19% in 2030.

717

## 718 **5 CONCLUSIONS**

719 Facing difficult challenges of severe urban and regional air pollution driven by swift economic  
720 development and enormous energy consumption, China has been implementing a series of policies in  
721 energy conservation and emission control since 2005. Although not specifically targeting Hg, a  
722 pollutant of broad international concern, the policies and measures have effectively constrained  
723 China's Hg emissions because of their ancillary effects. From 2005 to 2012, China's anthropogenic  
724 emissions of atmospheric Hg are estimated to have increased from 679 to 750 t, a much slower rate of  
725 growth than those of China's economy and energy consumption. The values are generally larger than  
726 those of global inventories, as higher activity levels (energy consumption and industrial production)  
727 and lower penetrations of emission control devices for certain industrial sources are applied in this  
728 study. Decreased Hg emissions are estimated for the JJJ, YRD, and PRD regions, the areas of the  
729 country with the highest density of population, economic activity, and energy consumption. The  
730 collective Hg emissions from four key sectors (power generation, cement production, iron & steel  
731 production, and nonferrous metal smelting) are estimated to decline 3% from 2005 to 2012, attributed  
732 to the enhanced use of devices with high energy efficiencies and pollutant removal rates. Even with  
733 considerable growth of energy use projected by IEA (2012), continued measures in pollution control  
734 will further constrain the national Hg emission trajectory in the future. Analyses that overlook the  
735 effects of recent energy and pollution control policies will thus likely result in overestimation of  
736 China's recent and future Hg emissions.

737 It should be noted, however, that the uncertainties of China's Hg emission estimate have at the  
738 same time increased in recent years. This is mainly because of high uncertainties about the operational  
739 and other characteristics of the same advanced APCDs or improved manufacturing technologies that  
740 are nevertheless believed to be reducing emissions in key sectors. In addition, the unknown levels and  
741 locations of illegal ASGM activities continue to contribute significantly to the uncertainty of China's  
742 Hg emissions. Beyond interest in the national Hg emission totals, the relatively poor understanding of  
743 the speciation of Hg by sector elevates the uncertainties of emissions of different species, which are of  
744 particular importance to scientists simulating atmospheric transport, chemistry, and the environmental  
745 fate of Hg. Given the ongoing dramatic changes of emission sources under current policies within the  
746 country, therefore, systematic investigations by sector are suggested for Hg pollution, to better track  
747 the variability of emission levels and efficiently reduce the uncertainty of emissions for all Hg species.  
748 Middle- to long-term observations of atmospheric Hg, both in polluted urban and regional background  
749 areas, are also needed to validate analyses of China's anthropogenic Hg emission and to confirm the  
750 beneficial effects of pollution control implementation in the country.

751

## 752 **ACKNOWLEDGEMENT**

753 This work was sponsored by the Natural Science Foundation of China (41205110), and by the  
754 Natural Science Foundation of Jiangsu (BK20140020 and BK2012310). We would like to thank  
755 Shuxiao Wang and Qingru Wu from Tsinghua University for providing detailed technology  
756 information on non-ferrous metal smelting, Simon Wilson from the Arctic Monitoring and  
757 Assessment Programme for providing information and data on emissions from artisanal gold mining,  
758 and Shigeru Suehiro from the International Energy Agency for providing data for Chinese energy and

759 industrial projections. Thanks also go to three anonymous reviewers for their very valuable comments  
760 to improve this work.

761

## 762 **REFERENCES**

763 AGC (Artisanal Gold Council), Global Database on Mercury Emissions from Artisanal and Small  
764 Scale Mining (ASGM), 2010. Available at: <http://www.mercurywatch.org>

765 AMAP/UNEP, 2013. Technical Background Report for the Global Mercury Assessment 2013. Arctic  
766 Monitoring and Assessment Programme, Oslo, Norway/UNEP Chemicals Branch, Geneva,  
767 Switzerland, 263 pp.

768 AMAP/UNEP, 2008. Technical Background Report to the Global Atmospheric Mercury Assessment.  
769 Arctic Monitoring and Assessment Programme, Oslo, Norway/UNEP Chemicals Branch, Geneva,  
770 Switzerland, 159 pp.

771 Bond, T. C., Streets, D. G., Yarber, K. F., Nelson, S. M., Woo, J. H., and Klimont, Z.: A  
772 technology-based global inventory of black and organic carbon emissions from combustion, J.  
773 Geophys. Res., 109, D14203, doi: 10.1029/2003jd003697, 2004.

774 Chen, C., Wang, H., Zhang, W., Hu, D., Chen, L., Wang, X.: High-resolution inventory of mercury  
775 emissions from biomass burning in China for 2000-2010 and a projection for 2020, J. Geophys. Res.,  
776 118, 12248-12256, 2013.

777 Chen, L., Liu, M., Fan, R., Ma, S., Xu, Z., Ren, M., He, Q.: Mercury speciation and emission from  
778 municipal solid waste incinerators in the Pearl River Delta, South China. Sci. Total Environ., 447,  
779 396-402, 2013.

780 Chen, Y., Wang, R., Shen, H., Li, W., Chen, H., Huang, Y., Zhang, Y., Chen, Y., Su, S., Lin, N., Liu,  
781 J., Li, B., Wang, X., Liu, W., Coveney, R. M., and Tao, S.: Global mercury emissions from  
782 combustion in light of international fuel trading, Environ. Sci. Technol., 48, 1727-1735, 2013.

783 China Association of Urban Environmental Sanitation (CAUES): Development Report on China  
784 Urban Environmental Sanitation (2012), China City Press, Beijing, 2013 (in Chinese).

785 Ci, Z., Zhang, X., Wang, Z.: Enhancing atmospheric mercury research in China to improve the  
786 current understanding of the global mercury cycle: the need for urgent and closely coordinated efforts,  
787 *Environ. Sci. Technol.*, 46, 5636-5642, 2012.

788 Corbitt, E. S., Jacob, D. J., Holmes, C. D., Streets, D. G., Sunderland, E. M.: Global source–receptor  
789 relationships for mercury deposition under present-day and 2050 emissions scenarios, *Environ. Sci.*  
790 *Technol.*, 45, 10477-10484, 2011.

791 Cui, X., Ma, L. P., Deng, C. L., Xu, W. J., Mao, N.: Research progress of removing mercury from  
792 coal-fired flue gas, *Chemical Industry and Engineering Progress*, 30, 1607-1612, 2011(in Chinese).

793 Driscoll, C. T., Mason, R. P., Chan, H. M., Jacob, D. J., and Pirrone, N.: Mercury as a global pollutant:  
794 sources, pathways, and effects. *Environ. Sci. Technol.*, 47, 4967-4983, 2013.

795 EMEP/EEA: EMEP/EEA CORINAIR emission inventory guidebook. Technical report No. 9/2009.  
796 European Environment Agency, 2009. Available at:  
797 <http://www.eea.europa.eu/publications/emep-eea-emission-inventory-guidebook-2009>

798 Feng, X., Streets, D. G., Hao, J., Wu, Y., Li, G.: Mercury emissions from industrial sources in China,  
799 In Pirrone, N., Mason, R. P. (Eds): *Mercury Fate and Transport in the Global Atmosphere*, Springer  
800 US, 67-79, 2009.

801 Feng, X., Li, G., Qiu, G.: A preliminary study on mercury contamination to the environment from  
802 artisanal zinc smelting using indigenous methods in Hezhang county, Guizhou, China-Part 1: mercury  
803 emission from zinc smelting and its influences on the surface waters, *Atmos. Environ.*, 38, 6223-6230,  
804 2004.

805 Feng, X., Sommer, J., Lindqvist, O., Hong, Y.: Occurrence, emissions and deposition of mercury  
806 during coal combustion in the province Guizhou, China, *Water Air Soil Pollut.*, 139, 311-324, 2002.

807 Frey, H. C., Zheng, J. Y.: Quantification of variability and uncertainty in air pollutant emission  
808 inventories: method and case study for utility NO<sub>x</sub> emissions, *J. Air & Waste Manage. Assoc.*, 52,  
809 1083-1095, 2002.

810 Fu, X., Feng, X., Sommar, J., Wang, S.: A review of studies on atmospheric mercury in China, *Sci.*  
811 *Total Environ.*, 421-422, 73-81, 2012a.

812 Fu, X., Feng, X., Shang, L., Wang, S., Zhang, H.: Two years of measurements of atmospheric total  
813 gaseous mercury (TGM) at a remote site in Mt. Changbai area, Northeastern China, *Atmos. Chem.*  
814 *Phys.*, 12, 4215-4226, 2012b.

815 Guo, Y., Yan, N., Yang, S., Qu, Z., Wu Z., Liu, Y., Liu, P., Jia, J.: Conversion of elemental mercury  
816 with a novel membrane delivery catalytic oxidation system, *Environ. Sci. Technol.*, 45, 706-711,  
817 2011.

818 Hao, C., Shen, Y., Zhang, Y.: Study on mercury consumption reduction plans for PVC resin industry  
819 in China, *Research of Environmental Sciences*, 18, 112-115, 2005 (in Chinese).

820 Hong, B., Zhu, Y., Feng, X., Wang, Y.: Distribution of mercury in coal gas generating procedure,  
821 *Earth and Environment*, 32, 12-16, 2004 (in Chinese).

822 Hu, D., Zhang, W., Chen, L., Chen, C., Ou, L., Tong, Y., Wei, W., Long, W., Wang, X.: Mercury  
823 emissions from waste combustion in China from 2004 to 2010, *Atmos. Environ.*, 62, 359-366, 2012.

824 Huang, W., Yang, Y.: Mercury in coal in China. *Coal Geology of China*, 14(S), 37-40, 2002 (in  
825 Chinese).

826 Huang, X., Li, M., Friedli, H. R. Song, Y., Chang, D., Zhu, L.: Mercury emissions from biomass  
827 burning in China, *Environ. Sci. Technol.*, 45, 9442-9448, 2011.

828 Huang, Y., Jin, B., Zhong, Z., Xiao, R.: Study on the distribution of trace elements in gasification  
829 products, *Proceedings of the CSEE*, 24, 208-212, 2004 (in Chinese).

830 International Energy Agency (IEA): *World Energy Outlook 2012*, International Energy Agency, Paris,  
831 France, 2012

832 Ito, S., Yokoyama, T., Asakura, K.: Emissions of mercury and other trace elements from coal-fired  
833 power plants in Japan, *Sci. Total Environ.*, 368, 397-402, 2006.

834 Lei, Y., Zhang, Q., Nielsen, C. P., He, K. B.: An inventory of primary air pollutants and CO<sub>2</sub>  
835 emissions from cement industry in China, 1990–2020, *Atmos. Environ.*, 45, 147-154, 2011.

836 Li, G., Feng, X., Li, Z., Qiu, G., Shang, L., Liang, P., Wang, D., Yang, Y.: Mercury emission to  
837 atmosphere from primary Zn production in China, *Sci. Total Environ.*, 408, 4607-4612, 2010.

838 Li, G., Feng, X., Li, Z.: Atmospheric mercury emissions from retort Zn productions, *J. Tsinghua Univ.*  
839 (Sci & Tech), 49, 2001-2004, 2009 (in Chinese).

840 Li, P., Feng, X., Qiu, G., Shang, L., Wang, S.: Mercury pollution in Wuchuan mercury mining area,  
841 Guizhou, Southwestern China: The impacts from large scale and artisanal mercury mining, *Environ.*  
842 *Int.*, 42, 59-66, 2012.

843 Li, P., Feng, X., Qiu, G., Shang, L., Wang, S., Meng, B.: Atmospheric mercury emission from  
844 artisanal mercury mining in Guizhou Province, Southwestern China, *Atmos. Environ.*, 43, 2247-2251,  
845 2009.

846 Li, W.: Characterization of Atmospheric Mercury Emissions from Coal-fired Power Plant and Cement  
847 Plant (Master Thesis), Xi'an University, Chongqing, China, 2011 (in Chinese).

848 Lin, C.-J., Pan, L., Streets, D. G., Shetty, S. K., Jang, C., Feng, X., Chu, H.-W., and Ho, T. C.:  
849 Estimating mercury emission outflow from East Asia using CMAQ-Hg, *Atmos. Chem. Phys.*, 10,  
850 1853-1864, 2010.

851 Muntean, M., Jassens-Maenhout, G., Song, S., Selin, N. E., Olivier, J. G. J., Guizzardi, D., Maas, R.,  
852 and Dentener, F.: Trend analysis from 1970 to 2008 and model evaluation of EDGARv4 global  
853 gridded anthropogenic mercury emissions, *Sci. Total Environ.*, 494-495, 337-350, 2014.

854 National Bureau of Statistics (NBS): China Statistical Yearbook 2005-2012, China Statistics Press,  
855 Beijing, 2013a (in Chinese).

856 National Bureau of Statistics (NBS): China Industry Economy Statistical Yearbook 2005-2012, China  
857 Statistics Press, Beijing, 2013b (in Chinese).

858 National Bureau of Statistics (NBS): China Statistical Yearbook 2005-2012, China Statistics Press,  
859 Beijing, 2013c (in Chinese).

860 Pacyna, E. G., Pacyna, J. M., Sundseth, K., Munthe, J., Kindbom, K., Wilson, S., Steenhuisen, F.,  
861 Maxson, P.: Global emission of mercury to the atmosphere from anthropogenic sources in 2005 and  
862 projections to 2020, *Atmos. Environ.*, 44, 2487-2499, 2010.

863 Pacyna, E. G., Pacyna, J. M.: Global emission of mercury from anthropogenic sources in 1995, *Water*  
864 *Air Soil Pollut.*, 137, 149-165, 2002.

865 Pan, L., Carmichael, G. R., Adhikary, B., Tang, Y., Streets, D. G., Woo, J. -H., Friedli, H. R., Radke,  
866 L. F.: A regional analysis of the fate and transport of mercury in East Asia and an assessment of major  
867 uncertainties, *Atmos. Environ.*, 42, 1144-1159, 2008.

868 Pan, L., Chai, T., Carmichael, G. R., Tang, Y., Streets, D., Woo, J. -H., Friedli, H. R., Radke, L. F.:  
869 Top-down estimate of mercury emissions in China using four-dimensional variational data  
870 assimilation, *Atmos. Environ.*, 41, 2804-2819, 2007.

871 Pirrone, N., Mason, R. P. (Eds): *Mercury fate and transport in the global atmosphere*, Springer US,  
872 2009.

873 Pirrone, N., Cinnirella, S., Feng, X., Finkelman, R. B., Friedli, H. R., Leaner, J., Mason, R.,  
874 Mukherjee, A. B., Stracher, G. B., Streets, D. G., Telmer, K.: Global mercury emissions to the  
875 atmosphere from anthropogenic and natural sources, *Atmos. Chem. Phys.*, 10, 5951-5964, 2010.

876 Rafaj, P., Bertok, I., Cofala, J., and Schopp, W.: Schopp, W.: Scenarios of global mercury emissions  
877 from anthropogenic sources, *Atmos. Environ.*, 79, 472-479, 2013.

878 Slemr, F., Brunke, E. G., Ebinghaus, R., Kuss, J.: Worldwide trend of atmospheric mercury since  
879 1995, *Atmos. Chem. Phys.*, 11, 4779-4787, 2011.

880 Srivastava, R K., Hutson, N., Martin, B., Princiotta, F., Staudt, J.: Control of mercury emissions from  
881 coal-fired electric utility boilers, *Environ. Sci. Technol.*, 40, 1385-1393, 2006.

882 Streets, D. G., Zhang, Q., Wu, Y.: Projections of global mercury emissions in 2050, *Environ. Sci.*  
883 *Technol.*, 43, 2983-2988, 2009a.

884 Streets, D. G., Hao, J., Wang, S., Wu, Y.: Mercury emissions from coal combustion in China, In  
885 Pirrone, N., Mason, R. P. (Eds): *Mercury Fate and Transport in the Global Atmosphere*, Springer US,  
886 51-65, 2009b.

887 Streets, D. G., Hao, J., Wu, Y., Jiang, J., Chan, M., Tian, H., Feng, X.: Anthropogenic mercury  
888 emissions in China, *Atmos. Environ.*, 39, 7789-7806, 2005.

889 Tang, S., Feng, X., Shang, L., Yan, H., Hou, Y.: Mercury speciation and emissions in the flue gas of a  
890 small-scale coal-fired boiler in Guiyang, *Research of Environmental Sciences*, 17, 74-76, 2004 (in  
891 Chinese).

892 Telmer K, Veiga M. World emissions of mercury from artisanal and small scale gold mining. In  
893 Pirrone, N., Mason, R. P. (Eds): *Mercury Fate and Transport in the Global Atmosphere*, Springer US,  
894 131-172, 2009.

895 Tian, H., Wang, Y., Cheng, K., Qu, Y., Hao, J, Xue, Z., Chai, F.: Control strategies of atmospheric  
896 mercury emissions from coal-fired power plants in China. *J. Air Waste Manag. Assoc.*, 62, 576-58,  
897 2012.

898 Tian, H. Z., Wang, Y., Xue, Z. G., Cheng, K., Qu, Y. P., Chai, F. H., Hao, J. M.: Trend and  
899 characteristics of atmospheric emissions of Hg, As, and Se from coal combustion in China,  
900 1980–2007, *Atmos. Chem. Phys.*, 10, 11905-11919, 2010.

901 Tsinghua University (THU): Improve the Estimates of Anthropogenic Mercury Emissions in China,  
902 Technical report, 2009. Available at: <http://ww.chem.unep.ch/MERCURY/>.

903 United Nations Economic Commission for Europe/The European Monitoring and Evaluation  
904 Programme (UNECE/EMEP): Atmospheric Emission Inventory Guidebook, 2004. Available at  
905 <http://reports.eea.eu.int/EMEP-CORINAIR4/en/page002.html>

906 U.S. Environmental Protection Agency (USEPA): Compilation of Air Pollutant Emission Factors  
907 (AP-42), 2002a. Available at <http://www.epa.gov/ttn/chief/ap42/index.html>.

908 U.S. Environmental Protection Agency (USEPA): Characterization and management of residues from  
909 coal-fired power plants, Interim Report, EPA-600/R-02-083, 2002b.

910 U. S. Geological Survey (USGS): Commodity Statistics and Information, 2011. Available at:  
911 <http://minerals.usgs.gov/minerals/pubs/commodity>.

912 U. S. Geological Survey (USGS): Mercury content in coal mines in China (unpublished data), 2004.

913 Wan, Q., Feng, X., Lu, J., Zheng, W., Song, X., Han, S., Xu, H.: Atmospheric mercury in Changbai  
914 Mountain area, northeastern China-Part 1: the seasonal distribution pattern of total gaseous mercury  
915 and its potential sources. *Environ. Res.*, 109:201-206, 2009.

916 Wang, F., The control policy for total emission amount of primary pollutants during the 12<sup>th</sup> Five  
917 Year Plan period, presented at the 17<sup>th</sup> Workshop on SO<sub>2</sub>, NO<sub>x</sub>, and Hg pollution control technology  
918 and PM<sub>2.5</sub> control and monitoring technology, Hangzhou, China, May 16-17, 2013.

919 Wang, K., Wang, C., Lu, X. D., Chen, J. N.: Scenario analysis on CO<sub>2</sub> emissions reduction potential  
920 in China's iron and steel industry, *Energy Policy*, 35, 2320-2335, 2007.

921 Wang, L., Wang, S., Zhang, L., Wang, Y., Zhang, Y., Nielsen, C., McElroy, M. B., Hao, J.: Source  
922 apportionment of atmospheric mercury pollution in China using the GEOS-Chem model, *Environ.*  
923 *Pollut.*, 190, 166-175, 2014.

- 924 Wang, Q., Shen, W., Ma, Z.: Estimation of mercury emission from coal combustion in China, *Environ.*  
925 *Sci. Technol.*, 34, 2711-2713, 2000
- 926 Wang, S. X., Zhang, L., Zhao, B., Meng, Y., Hao, J. M.: Mitigation potential of mercury emissions  
927 from coal-fired power plants in China, *Energy Fuels*, 26, 4635-4642, 2012.
- 928 Wang, S. X., Song, J. X., Li, G. H., Wu, Y., Zhang, L., Wan, Q., Streets, D. G., Chin, C. K., Hao, J.  
929 M.: Estimating mercury emissions from a zinc smelter in relation to China's mercury control policies,  
930 *Environ. Pollut.*, 158, 3347-3353, 2010a.
- 931 Wang, S. X., Zhang, L., Li, G. H., Wu, Y., Hao, J. M., Pirrone, N., Sprovieri, F., Ancora, M. P.:  
932 Mercury emission and speciation of coal-fired power plants in China, *Atmos. Chem. Phys.*, 10,  
933 1183-1192, 2010b.
- 934 Wang, S. X., Zhang, L., Wu, Y., Ancora, M. P., Yu Zhao, Hao, J. M.: Synergistic mercury removal by  
935 conventional pollutant control strategies for coal-fired power plants in China, *J. Air & Waste Manage.*  
936 *Assoc.*, 60, 722-730, 2010c.
- 937 Wang, W. X.: Analysis of energy consumption and energy saving potential for iron and steel industry,  
938 *China Steel*, 4, 19-22, 2011 (in Chinese).
- 939 Wu, Q. R., Wang, S. X., Zhang, L., Song, J. X., Yang, H., Meng, Y.: Update of mercury emissions  
940 from China's primary zinc, lead and copper smelters, 2000–2010. *Atmos. Chem. Phys.*, 12,  
941 11153-11163, 2012.
- 942 Wu, Y., Streets, D. G., Wang, S. X., Hao, J. M.: Uncertainties in estimating mercury emissions from  
943 coal-fired power plants in China, *Atmos. Chem. Phys.*, 10, 2937-2947, 2010.
- 944 Wu, Y., Wang, S., Streets, D. G., Hao, J., Chan, M., Jiang, J.: Trends in anthropogenic mercury  
945 emissions in China from 1995 to 2003, *Environ. Sci. Technol.*, 40, 5312-5318, 2006.
- 946 Xu, Y.: Improvements in the operation of SO<sub>2</sub> scrubbers in China's coal power plants, *Environ. Sci.*  
947 *Technol.*, 45, 380-385, 2011.
- 948 Yao, W., Qu, X., Li, H., Fu, Y.: Production, collection and treatment of garbage in rural areas in  
949 China, *J Environ Health*, 26, 10-12, 2009 (in Chinese).
- 950 Yan, N., Chen, W., Chen, J., Qu, Z., Guo, Y., Yan, S., Jia, J.: Significance of RuO<sub>2</sub> modified SCR  
951 catalyst for elemental mercury oxidation in coal-fired flue gas, *Environ. Sci. Technol.*, 45, 5725-5730,  
952 2011.

953 Zhang, L., Wang, S., Meng, Y., Hao, J.: Influence of mercury and chlorine content of coal on mercury  
954 emissions from coal-fired power plants in China, *Environ. Sci. Technol.*, 46, 6385-6392, 2012a.

955 Zhang, L., Wang, S., Wu, Q., Meng, Y., Yang, H., Wang, F., Hao, J.: Were mercury emission  
956 factors for Chinese non-ferrous metal smelters overestimated? Evidence from onsite measurements in  
957 six smelters, *Environ. Pollut.*, 171, 109-117, 2012b.

958 Zhang, L., Zhuo, Y., Chen, L., Xu X., Chen, C.: Mercury emissions from six coal-fired power plants  
959 in China, *Fuel Processing Technology.*, 89, 1033-1040, 2008.

960 Zhang, L.: Research on mercury emission measurement and estimate from combustion resources  
961 (Master Thesis), Zhejiang University, Hangzhou, China, 2007 (in Chinese).

962 Zhang, W., Wei, W., Hu, D., Zhu, Y., Wang, X.: Emission of speciated mercury from residential  
963 biomass fuel combustion in China, *Energy Fuels*, 27, 6792-6800, 2013.

964 Zhao, Y., Zhang, J., Nielsen, C. P.: The effects of energy paths and emission controls and standards  
965 on future trends in China's emissions of primary air pollutants, *Atmos. Chem. Phys.*, 14, 8849-8868,  
966 2014.

967 Zhao, Y., Zhang, J., Nielsen, C. P.: The effects of recent control policies on trends in emissions of  
968 anthropogenic atmospheric pollutants and CO<sub>2</sub> in China, *Atmos. Chem. Phys.*, 13, 487-508, 2013.

969 Zhao, Y., Nielsen, C. P., McElroy, M. B., Zhang, L., Zhang, J.: CO emissions in China: uncertainties  
970 and implications of improved energy efficiency and emission control, *Atmos. Environ.*, 49, 103-113,  
971 2012.

972 Zhao, Y., Nielsen, C. P., Lei, Y., McElroy, M. B., Hao, J. M.: Quantifying the uncertainties of a  
973 bottom-up emission inventory of anthropogenic atmospheric pollutants in China, *Atmos. Chem. Phys.*,  
974 11, 2295-2308, 2011.

975 Zhao, Y., Wang, S. X., Nielsen, C. P., Li, X. H., and Hao, J. M.: Establishment of a database of  
976 emission factors for atmospheric pollutants from Chinese coal-fired power plants, *Atmos. Environ.*,  
977 44, 1515-1523, 2010.

978 Zhao, Y., Wang, S. X., Duan, L., Lei, Y., Cao, P. F., Hao, J. M.: Primary air pollutant emissions of  
979 coal-fired power plants in China: current status and future prediction. *Atmos. Environ.*, 42, 8442-8452,  
980 2008.

981 Zhi, G., Xue, Z., Li, Y., Ma, J., Liu, Y., Meng, F., Chai, F.: Uncertainty of flue gas mercury emissions  
982 from coal-fired power plants in China based on field measurements, *Research of Environmental*  
983 *Sciences*, 26, 814-821, 2013 (in Chinese).

984 **FIGURE CAPTIONS**

985 **Figure 1. The penetrations of technologies and inter-annual trends of Hg emission factors for**  
986 **typical sources in China for 2005-2012 and S2 through 2030. In each panel, the left vertical axis**  
987 **indicates the percentages of various technologies and right vertical axis indicates the emission**  
988 **factors.**

989 **Figure 2. Mercury removal efficiencies of different APCD combinations estimated in this work,**  
990 **compared with other inventory studies.**

991 **Figure 3. National total Hg emissions with speciation from 2005 to 2012 and future trends under**  
992 **three scenarios through 2030. The error bars for 2005-2012 indicate the 95% confidence**  
993 **intervals of the annual total emission estimates. Estimates from other inventories are shown as**  
994 **well for comparison.**

995 **Figure 4. Provincial Hg emissions in 2010 and the relative changes between 2005 and 2012. The**  
996 **sizes of the pie graphs indicate absolute emissions by source in 2010. Emissions from ASGM are**  
997 **excluded.**

998 **Figure 5. (a) Relative changes in Hg emissions of the national total and different source**  
999 **categories, and (b) Relative changes of Hg emissions and activity levels for given sectors (all**  
1000 **values normalized to the levels in 2005)**

1001 **Figure 6. Comparison of current Hg emission estimates to those without updated time-variant**  
1002 **emission factors for (a) nonferrous metal smelting, (b) iron & steel production, (c) cement**  
1003 **production, and (d) solid waste incineration.**

1004 **Figure 7. Contribution of different parameters to variance of Hg emissions from CPP during**  
1005 **2005-2012.**

1006

## 1007 TABLES

1008 **Table 1 Uncertainties of Hg emission factors for main sources, expressed as the**  
1009 **probability distribution functions (PDF).**

| Parameters                                 | Samples       | Distribution <sup>a</sup> | Key characteristics for distribution functions |                                    |   |     |
|--|---------------|---------------------------|--|------------------------------------|---|-----|
|  |               |                           | P10 <sup>b</sup> /Min <sup>c</sup>             | P90 <sup>b</sup> /Max <sup>c</sup> | Mean <sup>b</sup> /Most likely <sup>c</sup> |     |
| Release rates of boilers for CPP, %        |               |                           |  |                                    |   |     |
| PC   | 32            | Triangular                | 89   | 100                                | 99  |     |
| Grate                                      | 2             | Triangular                | 92   | 100                                | 96  |     |
| CFB  | 3             | Triangular                | 93   | 100                                | 98  |     |
| Release rates of boilers for OIB/HB/FOS, % |               |                           |  |                                    |   |     |
| Grate                                      | 3             | Triangular                | 51   | 91                                 | 76  |     |
| CFB  | 1             | Triangular                | 51   | 100                                | 91  |     |
| Hg removal efficiency by APCDs for CPP, %  |               |                           |  |                                    |   |     |
| FF   | 5             | Weibull                   | 21   | 84                                 | 56  |     |
| ESP  | 44            | Normal                    | 18   | 23                                 | 20  |     |
| WET  | 3             | Weibull                   | 4  | 26                                 | 13  |     |
| FGD+ESP                                    | 30            | Weibull                   | 40   | 68                                 | 57  |     |
| CYC  | 3             | Uniform                   | 0  | 14                                 | -   |     |
| SCR  | 7             | Triangular                | 10   | 100                                | 77  |     |
| CFB+ESP                                    | 3             | Weibull                   | 18   | 60                                 | 43  |     |
| Nonferrous metal smelting <sup>d</sup>     |               |                           |  |                                    |   |     |
| Zinc                                       | EP            | 6                         | Triangular                                     | 0                                  | 45  | 9   |
|  | ISP           | 3                         | Uniform  | 0                                  | 140   | -   |
|  | RZSP          | 2                         | Uniform  | 2                                  | 38  | -   |
|  | AZSP          | 4                         | Triangular                                     | 4                                  | 203   | 89  |
| Lead                                       | RPSP          | 2                         | Uniform  | 0                                  | 1.4   | -   |
|  | SMP           | 2                         | Uniform  | 0                                  | 12  | -   |
| Copper                                     | FFSP          | 2                         | Uniform  | 0                                  | 0.3   | -   |
|  | RPSP          | 2                         | Uniform  | 0.1                                | 0.3   | -   |
| Cement production                          |               |                           |  |                                    |   |     |
| FF   | 7             | Weibull                   | 0.006  | 0.011                              | 0.008                                       |     |
| ESP  | 2             | Uniform                   | 0.01   | 0.11                               | -   |     |
| WET/CYC                                    | 2             | Uniform                   | 0.06   | 0.18                               | -   |     |
| Biofuel use/biomass open burning           |               |                           |  |                                    |   |     |
| Firewood                                   | 26            | Uniform                   | 0  | 50                                 | -   |     |
| Crops                                      | 9             | Uniform                   | 0  | 106                                | -   |     |
| Waste incineration                         |               |                           |  |                                    |   |     |
| Municipal                                  | 29            | Weibull                   | 0.21   | 0.32                               | 0.27  |     |
| Rural                                      | Release rates | 1                         | Normal   | 0.37                               | 0.63  | 0.5 |
|  | Hg content    | 31                        | Weibull  | 0.12                               | 1.58  | 0.6 |

1010 <sup>a</sup> Types of probability distributions:

1011 Triangular distribution: a continuous probability distribution based on a knowledge of the minimum  
1012 and maximum and an "inspired guess" as to the modal value;

1013 Weibull distribution: a continuous probability distribution described by equation

1014 
$$f(x) = \frac{\beta}{\eta} \left( \frac{x-\gamma}{\eta} \right)^{\beta-1} e^{-\left(\frac{x-\gamma}{\eta}\right)^\beta};$$

1015 Normal distribution: a continuous probability distribution described by the normal equation

1016 
$$f(x) = \frac{1}{\sigma\sqrt{2\pi}} e^{-\frac{(x-\mu)^2}{2\sigma^2}};$$

1017 Uniform distribution: a distribution that has constant probability within the given range.

1018 <sup>b</sup> P10 values mean that there is a probability of 10% that the actual result would be equal to or below  
1019 the P10 values; P50 mean that there is a probability of 50% that the actual result would be equal to or  
1020 below the P50 values; and P90 mean that there is a probability of 90% that the actual result would be  
1021 equal to or below the P90 values.

1022 <sup>c</sup> These values are for the minimum, the most likely, and the maximum values for the triangular  
1023 distribution function instead of P10, P50, and P90 values, or for the minimum and maximum values  
1024 for the uniform distribution function instead of P10 and P90 values.

1025 <sup>d</sup> Full names of manufacturing technologies: EP: electrolytic process; ISP: imperial smelting process;  
1026 RZSP: retort zinc smelting process; AZ: artisanal zinc smelting process; RPSP: rich-oxygen pool  
1027 smelting process; SMP: sinter machine process; and FFSP: flash furnace smelting process.

1028

1029 **Table 2 Uncertainties of mass fractions of Hg speciation for main source categories.**

| Parameters       |                  | Samples | Distribution         | Key characteristics for distribution functions / % |         |                  |
|------------------|------------------|---------|----------------------|--|---------|------------------|
|                  |                  |         |                      | P10/Min  | P90/Max | Mean/Most likely |
| FF               | Hg <sup>0</sup>  | 4       | Triangular           | 4.8  | 30.6    | 15.8             |
|                  | Hg <sup>p</sup>  | 4       | Triangular           | 0.0  | 34.8    | 10.8             |
| ESP              | Hg <sup>2+</sup> | 20      | Normal               | 27.9   | 42.4    | 35.2             |
|                  | Hg <sup>p</sup>  | 20      | Triangular           | 0.0  | 3.6     | 0.22             |
| FGD+ESP          | Hg <sup>2+</sup> | 11      | Normal               | 9.8  | 22.2    | 16.0             |
|                  | Hg <sup>p</sup>  | 11      | Triangular           | 0.0  | 3.7     | 0.3              |
| WET              | Hg <sup>0</sup>  | 2       | Uniform <sup>b</sup> | 0.0  | 60.0    | -                |
|                  | Hg <sup>p</sup>  | 2       | Uniform <sup>b</sup> | 0.0  | 28.0    | -                |
| NOC <sup>a</sup> | Hg <sup>0</sup>  | -       | Uniform <sup>b</sup> | 0.0  | 48.0    | -                |
|                  | Hg <sup>2+</sup> | -       | Uniform <sup>b</sup> | 0.0  | 40.0    | -                |
| SCR              | Hg <sup>2+</sup> | 6       | Triangular           | 15.7   | 40.6    | 27.6             |
| NMS_Zn           | Hg <sup>0</sup>  | 3       | Triangular           | 0.0  | 55.0    | 29.0             |
|                  | Hg <sup>p</sup>  | 3       | Uniform              | 0.0  | 5.0     | -                |
| NMS_Pb           | Hg <sup>2+</sup> | 2       | Triangular           | 15.0   | 65.0    | 40.0             |
| NMS_Cu           | Hg <sup>2+</sup> | 2       | Uniform              | 28.0   | 72.0    | -                |
| BIO              | Hg <sup>0</sup>  | 25      | Weibull              | 57.3   | 94.2    | 76.9             |
|                  | Hg <sup>2+</sup> | 25      | Triangular           | 0.0  | 21.7    | 5.0              |
| SWI              | Hg <sup>0</sup>  | 10      | Gamma                | 1.1  | 33.8    | 6.2              |
|                  | Hg <sup>p</sup>  | 10      | Gamma                | 0.1  | 2.6     | 0.5              |

1030 <sup>a</sup> No control device for coal combustion;

1031 <sup>b</sup> Tentatively assumed

1032 **Table 3 National Hg emissions by source category from 2005 to 2012.**

| Source category                            | 2005         | 2006         | 2007         | 2008         | 2009         | 2010         | 2011         | 2012         |
|--|--------------|--------------|--------------|--------------|--------------|--------------|--------------|--------------|
| <b>Coal-fired power plants</b>             | <b>144.7</b> | <b>149.5</b> | <b>152.5</b> | <b>144.2</b> | <b>140.6</b> | <b>140.0</b> | <b>155.8</b> | <b>143.6</b> |
| <b>Industry</b>                            | <b>473.0</b> | <b>495.9</b> | <b>530.0</b> | <b>533.8</b> | <b>546.0</b> | <b>542.3</b> | <b>540.3</b> | <b>526.4</b> |
| Cement production                          | 64.4         | 65.8         | 66.8         | 59.1         | 59.4         | 45.7         | 40.1         | 40.0         |
| Coal use                                   | 16.1         | 17.6         | 18.7         | 18.0         | 20.0         | 20.4         | 21.5         | 22.2         |
| Iron & steel plants                        | 26.2         | 28.0         | 28.2         | 29.7         | 32.3         | 34.8         | 36.8         | 37.6         |
| Heating boilers                            | 18.1         | 20.5         | 24.1         | 26.0         | 26.3         | 30.1         | 32.6         | 34.5         |
| Other industrial boilers                   | 61.2         | 66.7         | 76.0         | 81.6         | 83.7         | 80.6         | 87.9         | 87.4         |
| Nonferrous metal smelting                  | 87.4         | 98.1         | 114.2        | 108.1        | 112.7        | 117.6        | 105.1        | 91.4         |
| Zinc                                       | 43.0         | 49.0         | 58.3         | 59.2         | 63.4         | 72.2         | 69.9         | 68.1         |
| Lead                                       | 39.9         | 45.0         | 52.4         | 45.6         | 45.8         | 41.9         | 34.0         | 22.0         |
| Copper                                     | 4.5          | 4.1          | 3.4          | 3.4          | 3.5          | 3.5          | 1.2          | 1.4          |
| Gold mining                                | 184.4        | 183.8        | 183.8        | 182.3        | 183.3        | 179.5        | 181.0        | 182.6        |
| Large scale                                | 17.7         | 17.1         | 17.1         | 15.6         | 16.6         | 12.8         | 14.3         | 15.9         |
| Artisanal and small scale                  | 166.7        | 166.7        | 166.7        | 166.7        | 166.7        | 166.7        | 166.7        | 166.7        |
| Other miscellaneous processes              | 31.2         | 33.1         | 37.0         | 47.0         | 48.4         | 54.1         | 56.8         | 52.9         |
| Mercury mining                             | 16.2         | 13.5         | 14.2         | 23.7         | 25.3         | 28.2         | 28.3         | 24.0         |
| Battery/fluorescent lamp production        | 7.6          | 8.7          | 9.8          | 10.9         | 10.0         | 10.0         | 10.0         | 10.0         |
| PVC production                             | 7.0          | 8.8          | 10.7         | 10.0         | 10.7         | 13.6         | 16.0         | 16.3         |
| Oil and gas combustion                     | 0.5          | 2.1          | 2.3          | 2.3          | 2.4          | 2.4          | 2.6          | 2.6          |
| <b>Residential &amp; commercial sector</b> | <b>61.3</b>  | <b>59.8</b>  | <b>61.4</b>  | <b>63.6</b>  | <b>67.8</b>  | <b>70.7</b>  | <b>74.2</b>  | <b>79.5</b>  |
| Coal burning                               | 30.0         | 28.0         | 27.2         | 30.7         | 33.0         | 34.9         | 36.5         | 38.5         |
| Biofuel use/biomass open burning           | 10.3         | 10.5         | 9.7          | 9.2          | 9.4          | 8.2          | 8.3          | 8.4          |
| Solid waste incineration                   | 10.3         | 10.9         | 11.4         | 11.6         | 12.4         | 12.8         | 13.3         | 15.3         |
| Municipal                                  | 1.7          | 2.5          | 3.2          | 3.5          | 4.4          | 5.1          | 5.7          | 7.9          |
| Rural                                      | 8.6          | 8.4          | 8.2          | 8.1          | 7.9          | 7.7          | 7.6          | 7.4          |
| Oil and gas combustion                     | 10.7         | 10.4         | 13.1         | 12.1         | 13.0         | 14.9         | 16.1         | 17.4         |
| <b>Total</b>                               | <b>679.0</b> | <b>705.2</b> | <b>743.8</b> | <b>741.7</b> | <b>754.4</b> | <b>753.0</b> | <b>770.3</b> | <b>749.5</b> |
| <b>Total coal combustion</b>               | <b>296.2</b> | <b>310.2</b> | <b>326.6</b> | <b>330.3</b> | <b>335.9</b> | <b>340.7</b> | <b>371.1</b> | <b>363.8</b> |

1033

1034 **Table 4 Uncertainties of Hg emissions by sector for 2005, 2008, 2010 and 2012,**  
 1035 **expressed as the 95% confidence intervals of central estimates. The unit for**  
 1036 **emissions is metric tons (t).**

|                    | 2005             | 2008             | 2010             | 2012             |
|--------------------|------------------|------------------|------------------|------------------|
| CPP                | 145 (-48%, +73%) | 144 (-50%, +70%) | 140 (-51%, +77%) | 144 (-50%, +89%) |
| IND                | 473 (-30%, +43%) | 534 (-27%, +46%) | 543 (-26%, +51%) | 527 (-27%, +54%) |
| RES                | 61 (-36%, +144%) | 64 (-35%, +127%) | 71 (-34%, +123%) | 79 (-35%, +115%) |
| Total              | 679 (-26%, +46%) | 742 (-24%, +46%) | 753 (-23%, +51%) | 750 (-23%, +53%) |
| Total <sup>a</sup> | 512 (-25%, +55%) | 575 (-24%, +56%) | 586 (-23%, +61%) | 583 (-24%, +65%) |
| Coal               | 296 (-48%, +70%) | 330 (-49%, +66%) | 341 (-49%, +69%) | 364 (-48%, +76%) |

1037 <sup>a</sup> Emissions from ASGM excluded.

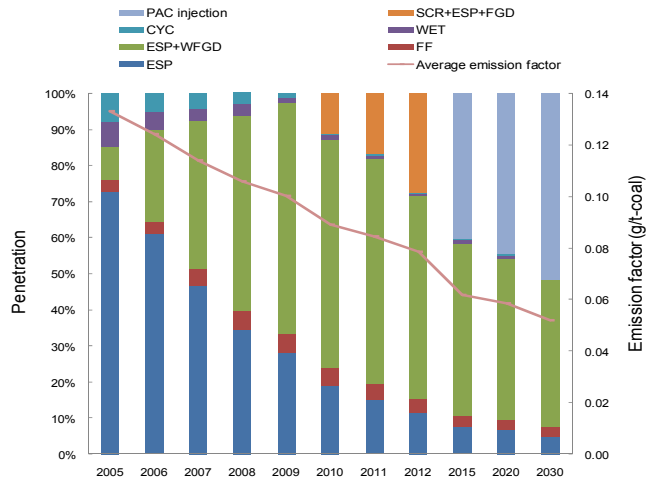
1038 **Table 5 The parameters contributing most to emission uncertainties by sector for**  
 1039 **2010. The percentages in the parentheses indicate the contributions of the**  
 1040 **parameters to the variance of corresponding emission estimates.**

|                  | CPP                          | IND                      | RES                     |
|------------------|------------------------------|--------------------------|-------------------------|
| Hg               | $\eta_{ESP+FGD}$ (26%)       | $E_{ASGM}$ (41%)         | $EF_{straw}$ (26%)      |
|                  | $HgC_{Shandong}$ (21%)       | $EF_{NMS\_Zn, EP}$ (17%) | $AL_{coal}$ (14%)       |
| Hg <sup>0</sup>  | $HgC_{Shandong}$ (18%)       | $E_{ASGM}$ (39%)         | $EF_{straw}$ (41%)      |
|                  | $HgC_{Henan}$ (8%)           | $f_{GM, Hg^{2+}}$ (19%)  | $AL_{straw}$ (12%)      |
| Hg <sup>2+</sup> | $HgC_{Shandong}$ (20%)       | $f_{GM, Hg^{2+}}$ (28%)  | $HgC_{waste}$ (28%)     |
|                  | $f_{ESP+FGD, Hg^{2+}}$ (13%) | $EF_{NMS\_Zn, EP}$ (22%) | $f_{NOC, Hg^{2+}}$ (8%) |
| Hg <sup>p</sup>  | $f_{ESP+FGD, Hgp}$ (30%)     | $f_{WET, Hgp}$ (74%)     | $AL_{coal}$ (22%)       |
|                  | $f_{FF, Hgp}$ (14%)          | $HgC_{Shandong}$ (4%)    | $f_{NOC, Hg^0}$ (15%)   |

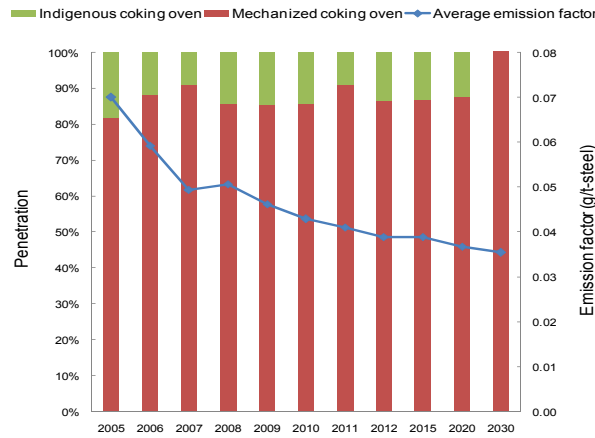
1041 **Table 6 Projected national Hg emissions by source category for different scenarios**  
 1042 **through 2030.**

| Source category                            | 2015         |              |              | 2020         |              |              | 2030         |              |              |
|--|--------------|--------------|--------------|--------------|--------------|--------------|--------------|--------------|--------------|
|  | S0           | S1           | S2           | S0           | S1           | S2           | S0           | S1           | S2           |
| <b>Coal-fired power plants</b>             | <b>150.0</b> | <b>149.6</b> | <b>130.8</b> | <b>164.2</b> | <b>153.1</b> | <b>130.9</b> | <b>181.8</b> | <b>155.0</b> | <b>126.8</b> |
| <b>Industry</b>                            | <b>578.1</b> | <b>571.1</b> | <b>405.4</b> | <b>588.0</b> | <b>580.9</b> | <b>401.4</b> | <b>570.9</b> | <b>547.6</b> | <b>342.5</b> |
| Cement production                          | 36.8         | 36.6         | 25.4         | 37.5         | 37.3         | 17.2         | 25.0         | 24.3         | 8.9          |
| Coal use                                   | 21.1         | 21.0         | 13.2         | 21.7         | 21.6         | 11.3         | 17.6         | 17.3         | 8.7          |
| Iron & steel plants                        | 40.0         | 39.9         | 39.3         | 41.7         | 41.4         | 39.0         | 39.8         | 39.1         | 34.8         |
| Heating boilers                            | 39.2         | 37.8         | 34.2         | 38.8         | 37.4         | 33.8         | 40.8         | 36.1         | 32.3         |
| Other industrial boilers                   | 105.2        | 101.3        | 86.4         | 104.1        | 100.4        | 85.4         | 109.4        | 96.8         | 81.7         |
| Nonferrous metal smelting                  | 110.5        | 109.6        | 102.4        | 116.0        | 115.0        | 105.5        | 109.6        | 106.8        | 68.2         |
| Zinc                                       | 84.5         | 83.8         | 78.9         | 88.7         | 88.0         | 81.8         | 83.8         | 81.7         | 56.0         |
| Lead                                       | 24.7         | 24.5         | 22.3         | 25.9         | 25.7         | 22.4         | 24.5         | 23.9         | 11.0         |
| Copper                                     | 1.3          | 1.3          | 1.2          | 1.4          | 1.3          | 1.3          | 1.3          | 1.3          | 1.2          |
| Gold mining                                | 182.5        | 182.4        | 63.3         | 183.3        | 183.1        | 63.7         | 182.4        | 182.0        | 63.2         |
| Large scale                                | 15.5         | 15.4         | 7.7          | 16.3         | 16.1         | 8.1          | 15.4         | 15.0         | 7.5          |
| Artisanal and small scale                  | 167.0        | 167.0        | 55.7         | 167.0        | 167.0        | 55.7         | 167.0        | 167.0        | 55.7         |
| Other miscellaneous processes              | 64.0         | 63.5         | 54.3         | 66.6         | 66.1         | 56.7         | 63.9         | 62.6         | 53.4         |
| Mercury mining                             | 34.1         | 33.8         | 33.8         | 35.8         | 35.5         | 35.5         | 33.8         | 33.0         | 33.0         |
| Battery/fluorescent lamp production        | 10.0         | 10.0         | 3.3          | 10.0         | 10.0         | 3.3          | 10.0         | 10.0         | 3.3          |
| PVC production                             | 16.8         | 16.7         | 14.1         | 17.7         | 17.5         | 14.8         | 16.7         | 16.3         | 13.7         |
| Oil and gas combustion                     | 3.0          | 3.0          | 3.0          | 3.2          | 3.1          | 3.1          | 3.3          | 3.3          | 3.3          |
| <b>Residential &amp; commercial sector</b> | <b>86.0</b>  | <b>84.2</b>  | <b>84.2</b>  | <b>92.0</b>  | <b>88.4</b>  | <b>88.4</b>  | <b>116.7</b> | <b>109.9</b> | <b>109.9</b> |
| Coal burning                               | 37.9         | 37.0         | 37.0         | 37.3         | 36.4         | 36.4         | 34.6         | 31.6         | 31.5         |
| Biofuel use/biomass open burning           | 8.7          | 8.7          | 8.7          | 8.1          | 8.1          | 8.1          | 6.6          | 6.6          | 6.6          |
| Solid waste incineration                   | 20.7         | 20.7         | 20.7         | 24.6         | 24.6         | 24.6         | 49.7         | 49.7         | 49.7         |
| Municipal                                  | 13.9         | 13.9         | 13.9         | 18.5         | 18.5         | 18.5         | 45.1         | 45.1         | 45.1         |
| Rural                                      | 6.8          | 6.8          | 6.8          | 6.1          | 6.1          | 6.1          | 4.6          | 4.6          | 4.6          |
| Oil and gas combustion                     | 18.7         | 17.8         | 17.8         | 22.0         | 19.3         | 19.3         | 25.8         | 22.0         | 22.0         |
| <b>Total</b>                               | <b>814.1</b> | <b>805.0</b> | <b>620.4</b> | <b>844.3</b> | <b>822.5</b> | <b>620.7</b> | <b>869.3</b> | <b>812.5</b> | <b>579.1</b> |
| <b>Total coal combustion</b>               | <b>393.3</b> | <b>386.7</b> | <b>340.9</b> | <b>407.9</b> | <b>390.4</b> | <b>336.9</b> | <b>423.9</b> | <b>375.9</b> | <b>315.8</b> |

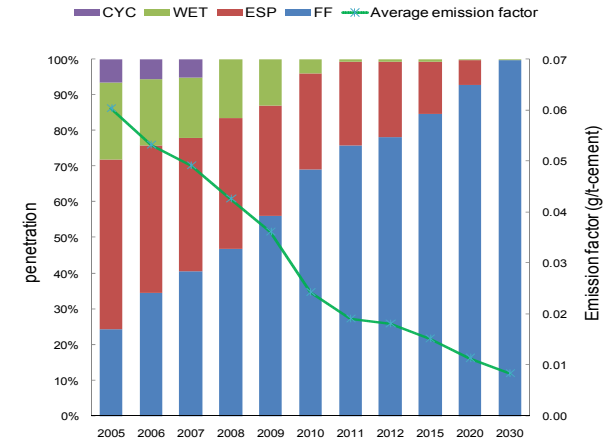
**Figure 1**



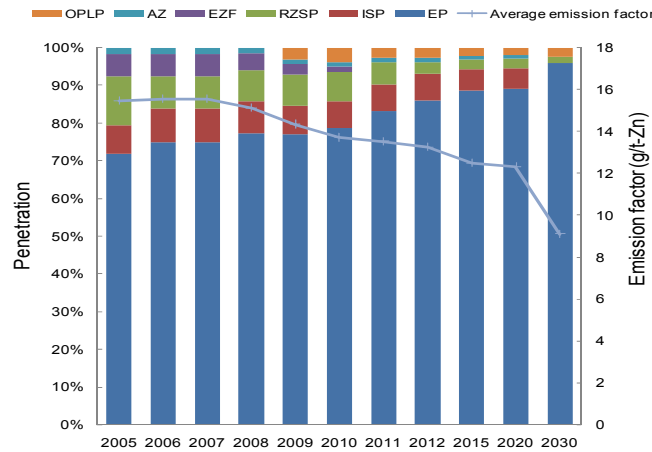
(a) Coal-fired power plants



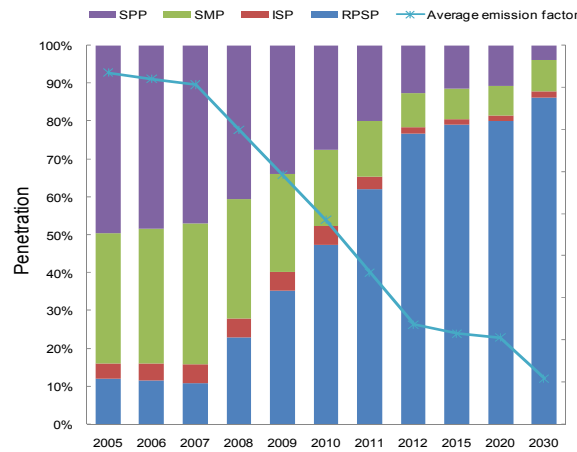
(b) Iron & steel production



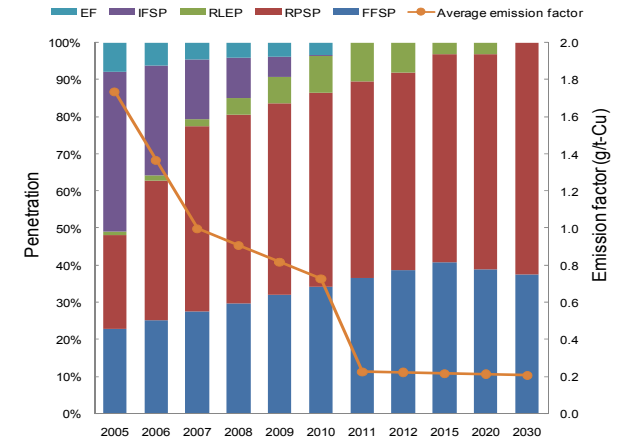
(c) Cement production



(d) Zn smelting



(e) Pb smelting



(f) Cu smelting

**Figure 2**

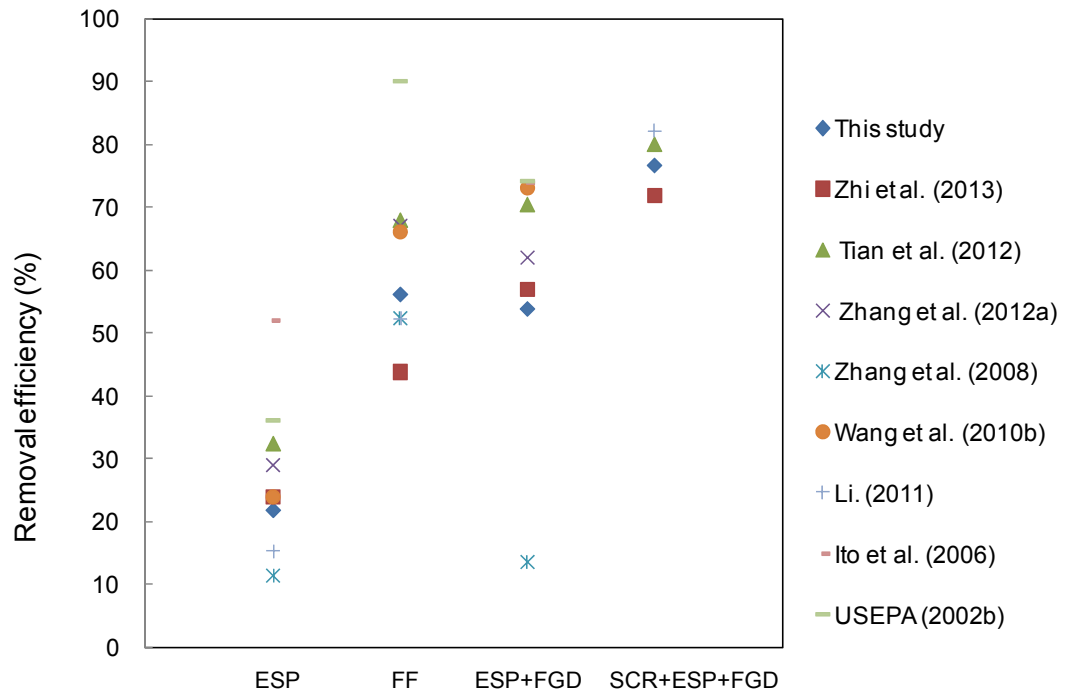


**Figure 3**

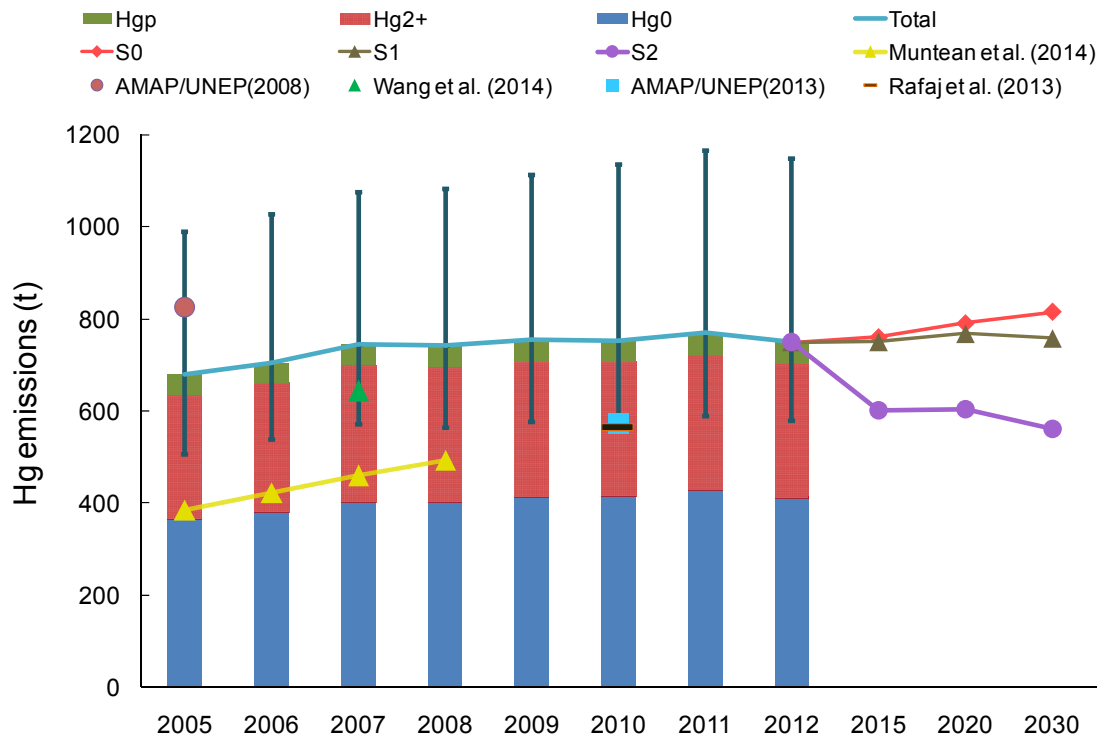


**Figure 4**

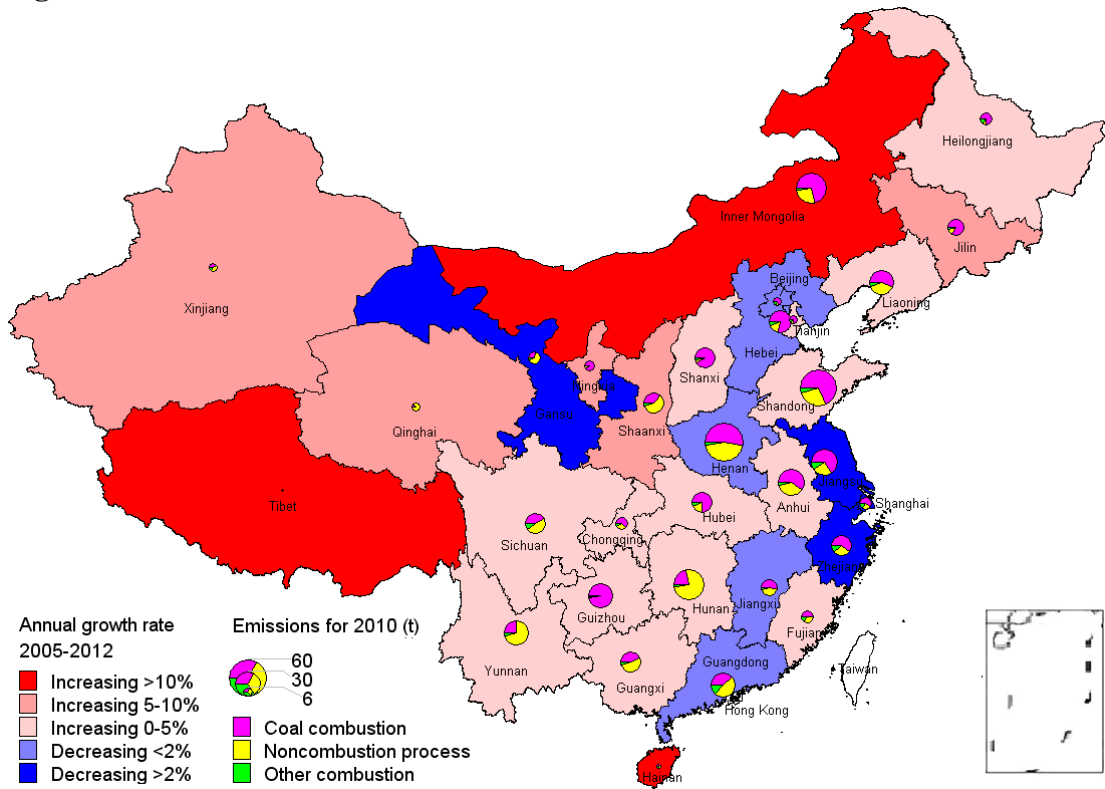
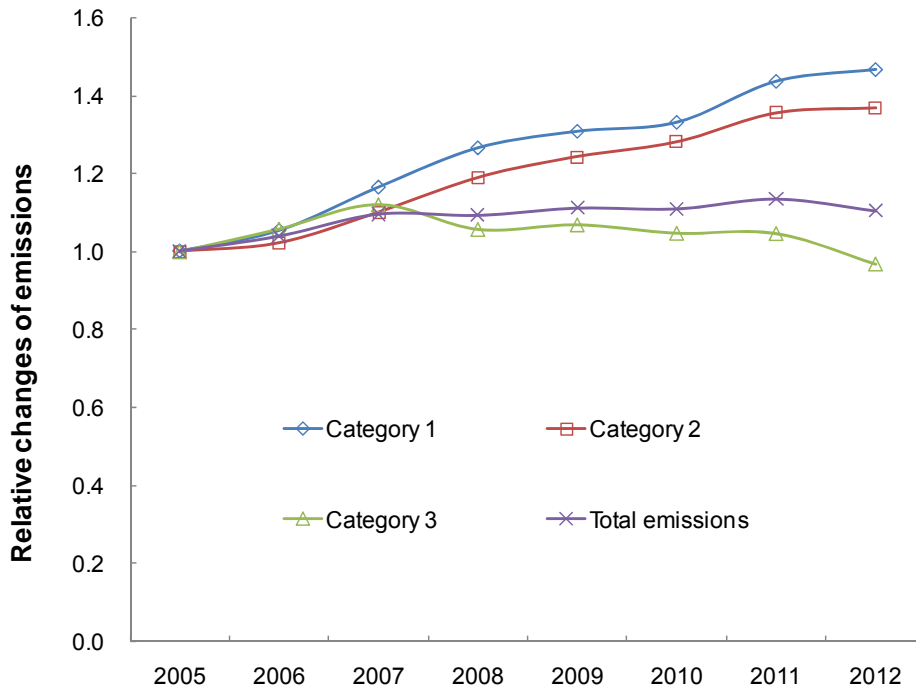
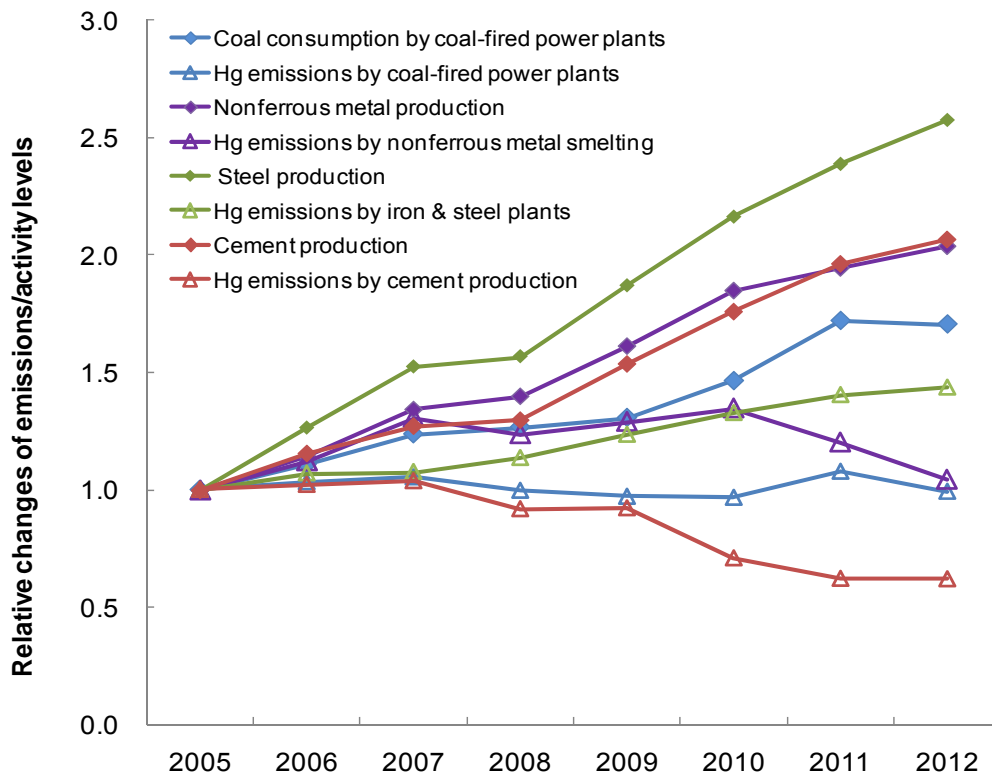


Figure 5

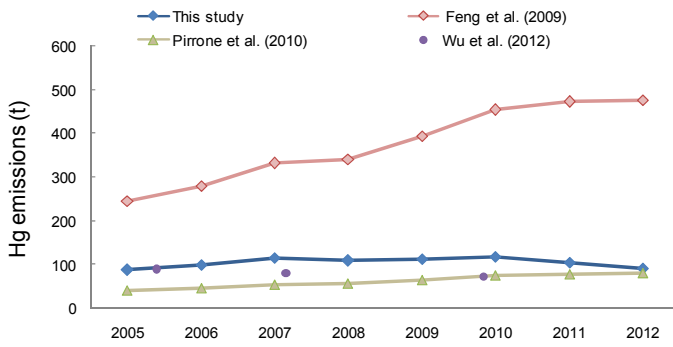


(a)

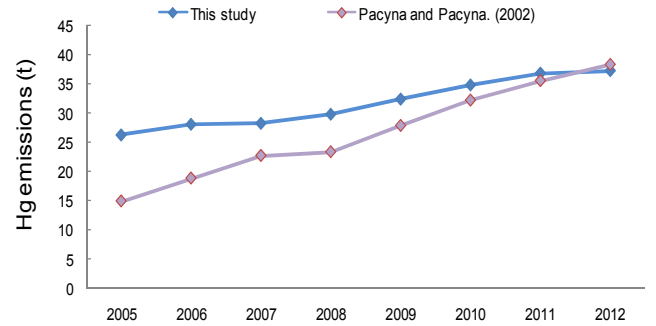


(b)

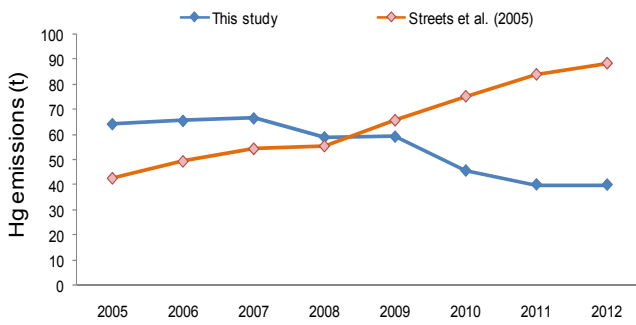
**Figure 6**



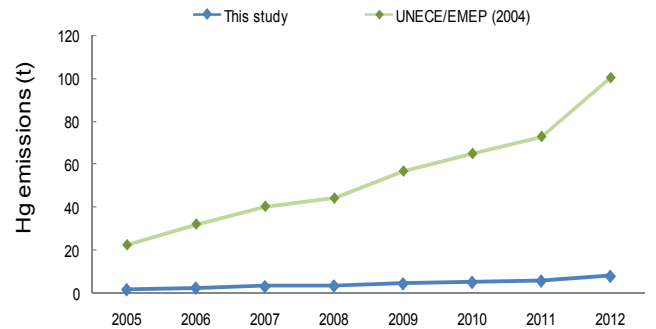
(a) Non-ferrous metal smelting



(b) Iron & steel production



(c) Cement production



(d) Municipal waste incineration

Notes: all the estimates of cited studies except Wu et al. (2012) are not directly obtained from the literatures, but calculated based on the same emission factors suggested by those studies.

**Figure 7**

